Light nuclei in the Fermionic Molecular Dynamics approach

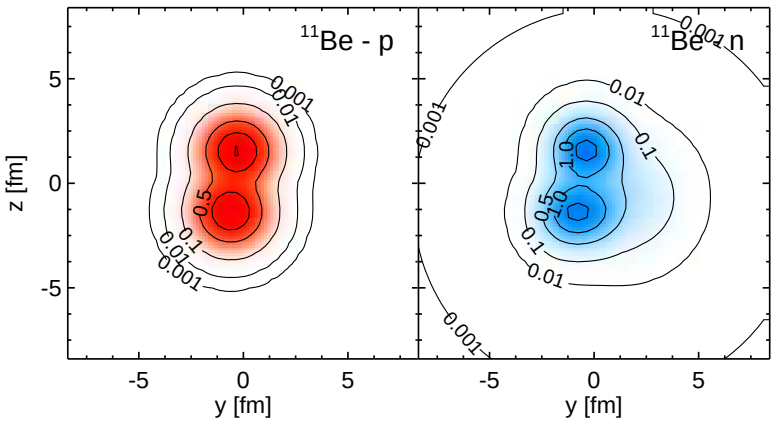

Thomas Neff

6th ANL/MSU/JINA/INT FRIB Theory Workshop

Argonne Natl Lab, USA
March 25, 2010

HELMHOLTZ ASSOCIATION

GSI

Overview

Effective Nucleon-Nucleon interaction:

Unitary Correlation Operator Method

Roth, Neff, Feldmeier, arXiv:1003.3624

- **Short-range Correlations**
- **Correlated Interaction**
- ***ab initio* Few- and Many-Body Calculations**

Many-Body Method:

Fermionic Molecular Dynamics

- **Model**
- **Beryllium Isotopes**
- **Cluster States in ^{12}C**

Nuclear Force

Argonne V18 (T=0)

spins aligned parallel or perpendicular to the relative distance vector

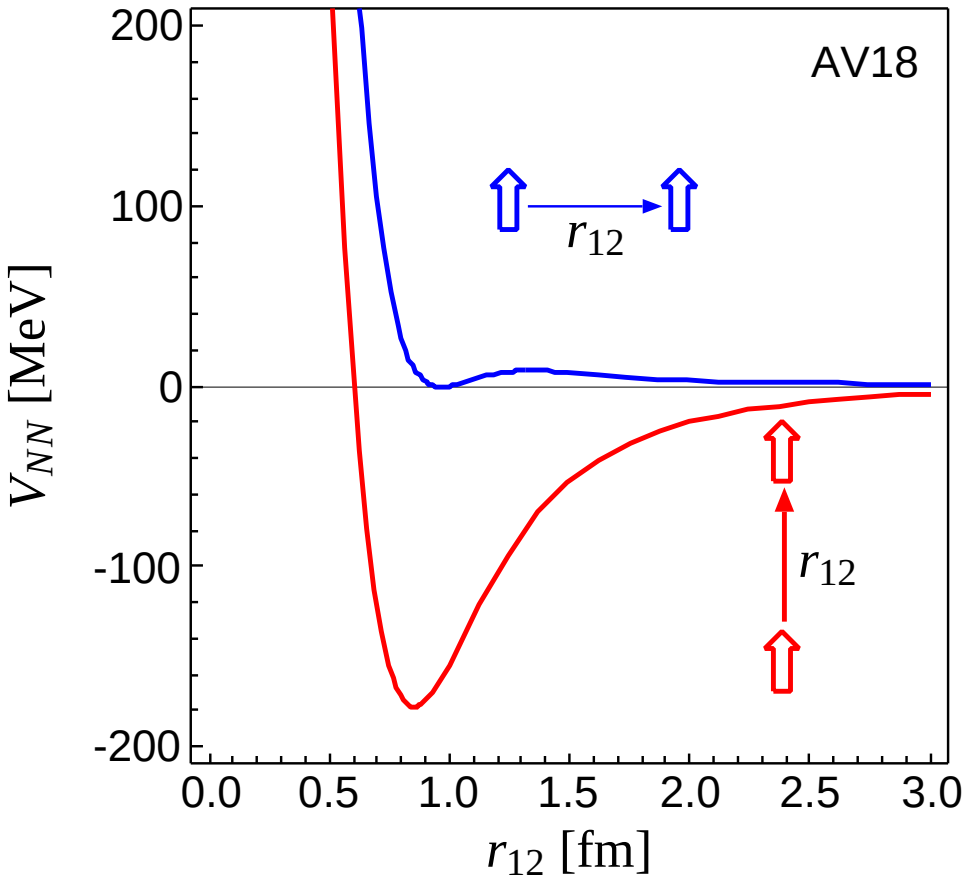

- strong repulsive core: nucleons can not get closer than ≈ 0.5 fm

➨ **central correlations**

- strong dependence on the orientation of the spins due to the tensor force

➨ **tensor correlations**

Nuclear Force

Argonne V18 (T=0)

spins aligned parallel or perpendicular to the relative distance vector

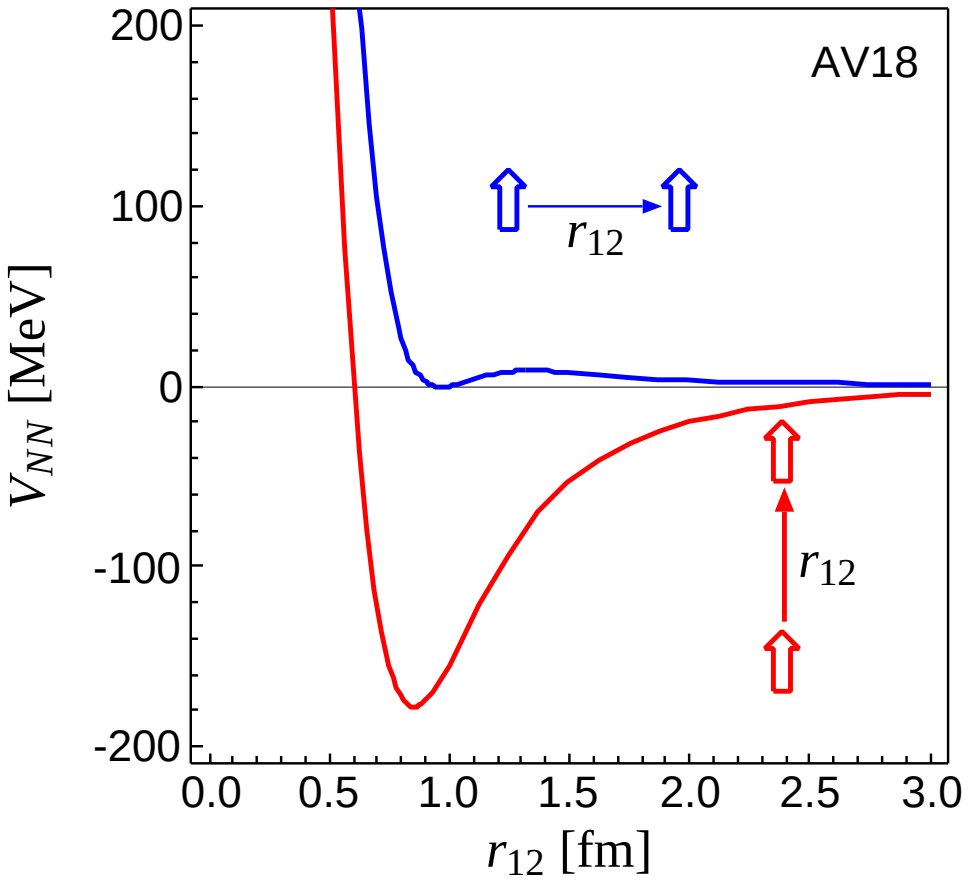

- strong repulsive core: nucleons can not get closer than ≈ 0.5 fm

➨ **central correlations**

- strong dependence on the orientation of the spins due to the tensor force

➨ **tensor correlations**

the nuclear force will induce **strong short-range correlations** in the nuclear wave function

UCOM

Unitary Correlation Operator Method

Correlation Operator

- induce short-range (two-body) central and tensor correlations into the many-body state

$$\underset{\sim}{C} = \underset{\sim}{C}_\Omega \underset{\sim}{C}_r = \exp\Big[-i \sum_{i<j} \underset{\sim}{g}_{\Omega,ij}\Big] \exp\Big[-i \sum_{i<j} \underset{\sim}{g}_{r,ij}\Big] \quad , \quad \underset{\sim}{C}^\dagger \underset{\sim}{C} = \underset{\sim}{1}$$

- correlation operator should conserve the symmetries of the Hamiltonian and should be of finite-range, correlated interaction **phase shift equivalent** to bare interaction by construction

Correlated Operators

- correlated operators will have contributions in higher cluster orders

$$\underset{\sim}{C}^\dagger \underset{\sim}{O} \underset{\sim}{C} = \underset{\sim}{\hat{O}}^{[1]} + \underset{\sim}{\hat{O}}^{[2]} + \underset{\sim}{\hat{O}}^{[3]} + \ldots$$

- two-body approximation: correlation range should be small compared to mean particle distance

Correlated Interaction

$$\underset{\sim}{C}^\dagger (\underset{\sim}{T} + \underset{\sim}{V}) \underset{\sim}{C} = \underset{\sim}{T} + \underset{\sim}{V}_{\mathrm{UCOM}} + \underset{\sim}{V}^{[3]}_{\mathrm{UCOM}} + \ldots$$

UCOM

Central and Tensor Correlations

$$\underset{\sim}{C} = \underset{\sim}{C}_\Omega \underset{\sim}{C}_r$$

$$\mathbf{p} = \mathbf{p}_r + \mathbf{p}_\Omega$$

$$\mathbf{p}_r = \frac{1}{2}\left\{\frac{\mathbf{r}}{r}\left(\frac{\mathbf{r}}{r}\mathbf{p}\right) + \left(\mathbf{p}\frac{\mathbf{r}}{r}\right)\frac{\mathbf{r}}{r}\right\}, \qquad \mathbf{p}_\Omega = \frac{1}{2r}\left\{\mathbf{l}\times\frac{\mathbf{r}}{r} - \frac{\mathbf{r}}{r}\times\mathbf{l}\right\}$$

UCOM

Central and Tensor Correlations

$$\underset{\sim}{C} = \underset{\sim}{C}_\Omega \underset{\sim}{C}_r$$

$$\mathbf{p} = \mathbf{p}_r + \mathbf{p}_\Omega$$

$$\mathbf{p}_r = \frac{1}{2}\left\{\frac{\mathbf{r}}{r}\left(\frac{\mathbf{r}}{r}\mathbf{p}\right) + \left(\mathbf{p}\frac{\mathbf{r}}{r}\right)\frac{\mathbf{r}}{r}\right\}, \qquad \mathbf{p}_\Omega = \frac{1}{2r}\left\{\mathbf{l}\times\frac{\mathbf{r}}{r} - \frac{\mathbf{r}}{r}\times\mathbf{l}\right\}$$

Central Correlations

$$\underset{\sim}{c}_r = \exp\left\{-\frac{i}{2}\{p_r s(r) + s(r) p_r\}\right\}$$

- probability density shifted out of the repulsive core

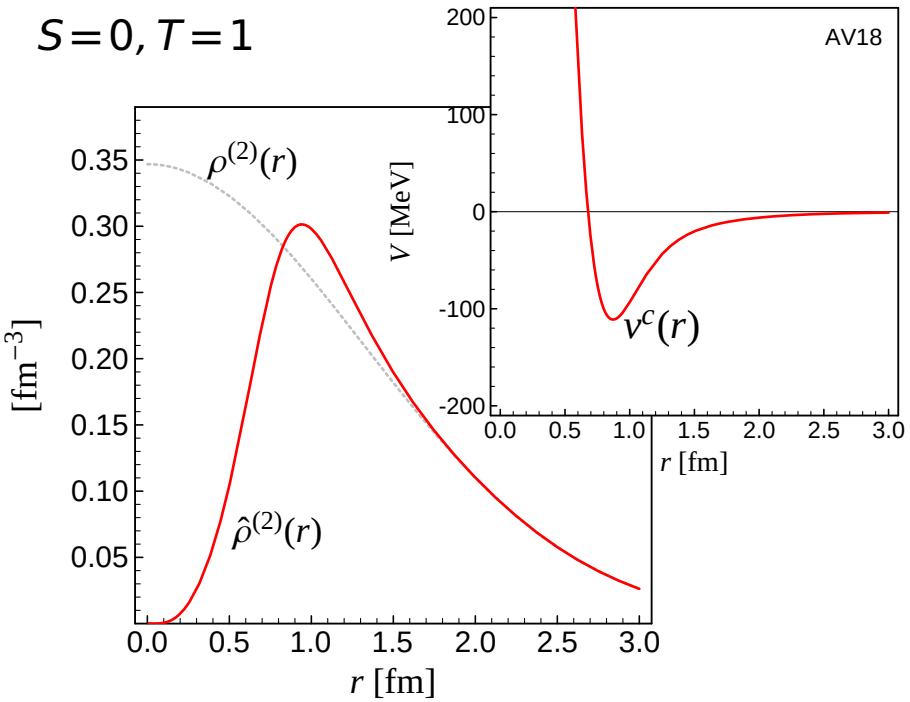

UCOM

Central and Tensor Correlations

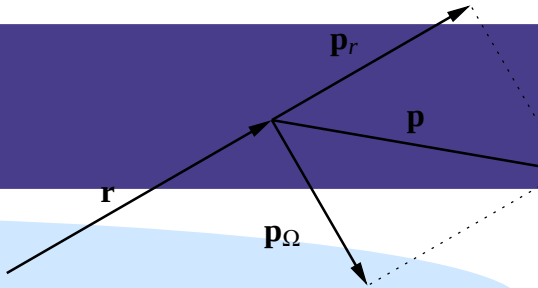

$$\underset{\sim}{C} = \underset{\sim}{C}_\Omega \underset{\sim}{C}_r$$

$$\mathbf{p} = \mathbf{p}_r + \mathbf{p}_\Omega$$

$$\mathbf{p}_r = \tfrac{1}{2}\left\{\frac{\mathbf{r}}{r}\left(\frac{\mathbf{r}}{r}\mathbf{p}\right) + \left(\mathbf{p}\frac{\mathbf{r}}{r}\right)\frac{\mathbf{r}}{r}\right\}, \qquad \mathbf{p}_\Omega = \frac{1}{2r}\left\{\mathbf{l}\times\frac{\mathbf{r}}{r} - \frac{\mathbf{r}}{r}\times\mathbf{l}\right\}$$

Central Correlations

$$\underset{\sim}{c}_r = \exp\left\{-\tfrac{i}{2}\{p_r s(r) + s(r) p_r\}\right\}$$

- probability density shifted out of the repulsive core

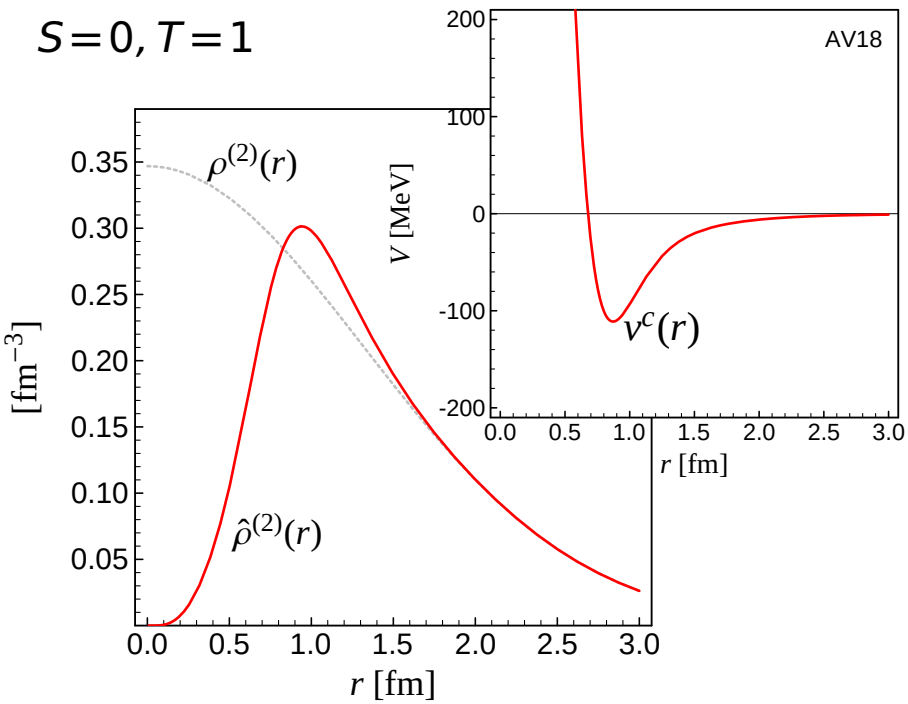

Tensor Correlations

$$\underset{\sim}{c}_\Omega = \exp\left\{-i\vartheta(r)\left\{\tfrac{3}{2}(\boldsymbol{\sigma}_1\cdot\mathbf{p}_\Omega)(\boldsymbol{\sigma}_2\cdot\mathbf{r}) + \tfrac{3}{2}(\boldsymbol{\sigma}_1\cdot\mathbf{r})(\boldsymbol{\sigma}_2\cdot\mathbf{p}_\Omega)\right\}\right.$$

- tensor force admixes other angular momenta

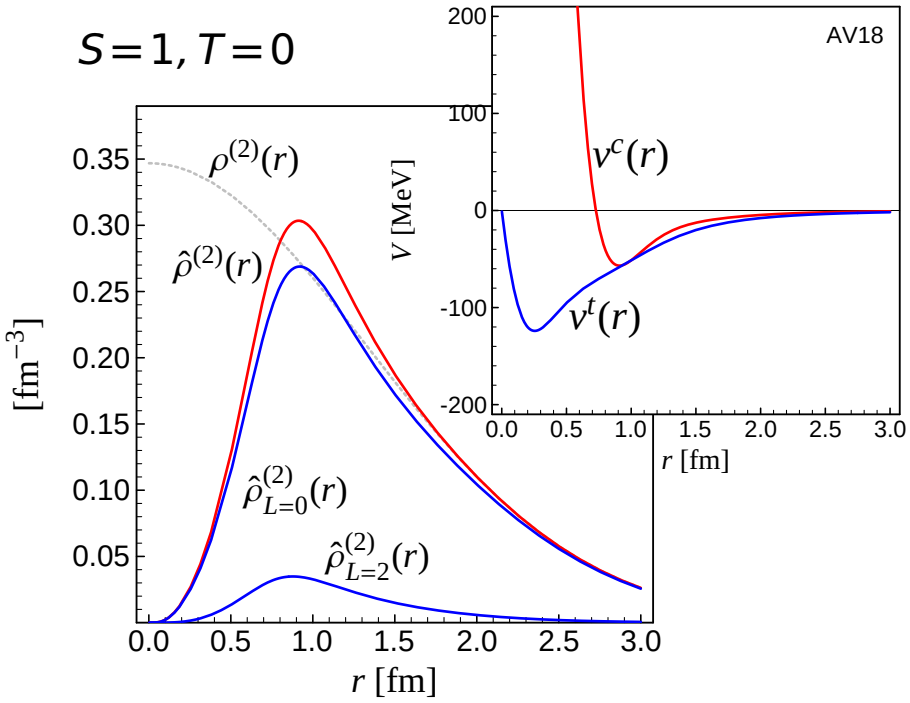

UCOM

Central and Tensor Correlations

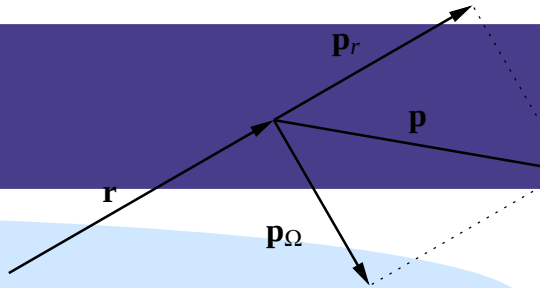

$$\underset{\sim}{C} = \underset{\sim}{C}_\Omega \underset{\sim}{C}_r$$

$$\mathbf{p} = \mathbf{p}_r + \mathbf{p}_\Omega$$

$$\mathbf{p}_r = \tfrac{1}{2}\left\{\frac{\mathbf{r}}{r}\left(\frac{\mathbf{r}}{r}\mathbf{p}\right) + \left(\mathbf{p}\frac{\mathbf{r}}{r}\right)\frac{\mathbf{r}}{r}\right\}, \qquad \mathbf{p}_\Omega = \frac{1}{2r}\left\{\mathbf{l}\times\frac{\mathbf{r}}{r} - \frac{\mathbf{r}}{r}\times\mathbf{l}\right\}$$

Central Correlations

$$\underset{\sim}{c}_r = \exp\left\{-\tfrac{i}{2}\{p_r s(r) + s(r) p_r\}\right\}$$

- probability density shifted out of the repulsive core

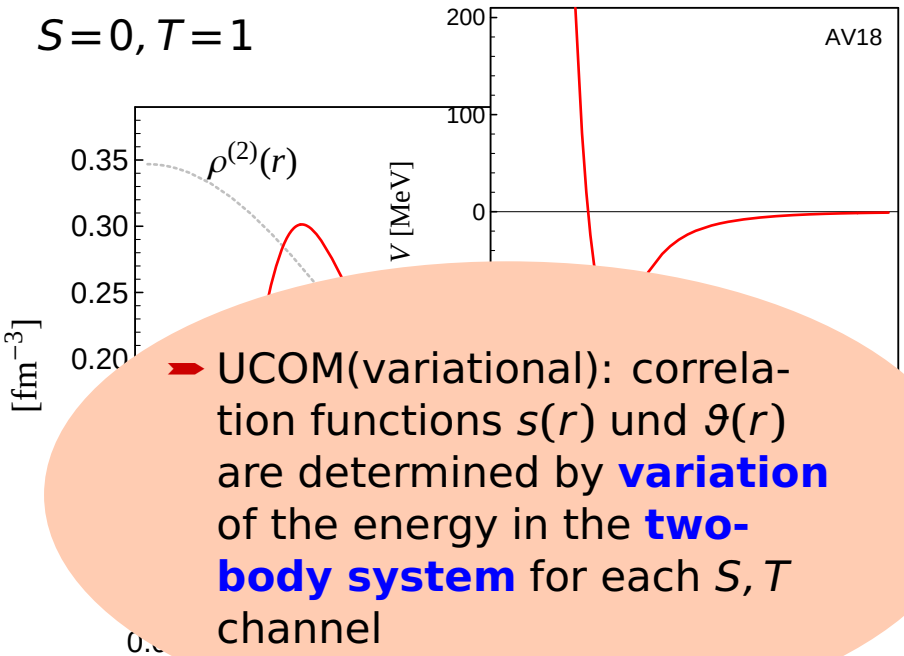

- UCOM(variational): correlation functions $s(r)$ und $\vartheta(r)$ are determined by **variation** of the energy in the **two-body system** for each S, T channel

Tensor Correlations

$$\underset{\sim}{c}_\Omega = \exp\left\{-i\vartheta(r)\left\{\tfrac{3}{2}(\boldsymbol{\sigma}_1\cdot\mathbf{p}_\Omega)(\boldsymbol{\sigma}_2\cdot\mathbf{r}) + \tfrac{3}{2}(\boldsymbol{\sigma}_1\cdot\mathbf{r})(\boldsymbol{\sigma}_2\cdot\mathbf{p}_\Omega)\right\}\right.$$

- tensor force admixes other angular momenta

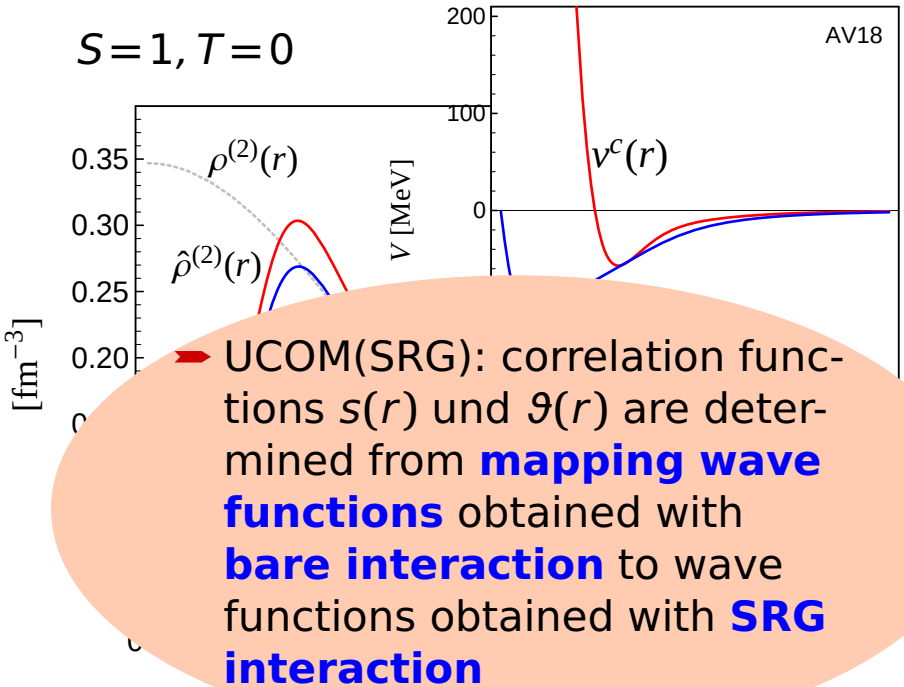

- UCOM(SRG): correlation functions $s(r)$ und $\vartheta(r)$ are determined from **mapping wave functions** obtained with **bare interaction** to wave functions obtained with **SRG interaction**

Realistic Effective Interaction

two-body densities

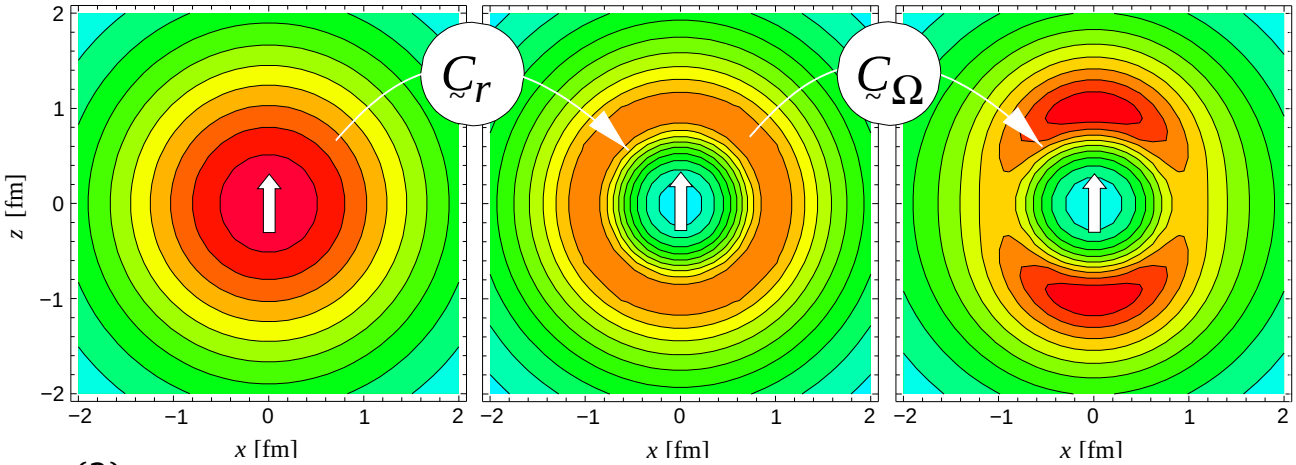

$\rho^{(2)}_{S,T}(\mathbf{r}_1 - \mathbf{r}_2) \quad S = 1, M_S = 1, T = 0$

central correlator $\hat{C}_r$ shifts density out of the repulsive core

tensor correlator $\hat{C}_\Omega$ aligns density with spin orientation

Neff and Feldmeier, Nucl. Phys. **A713** (2003) 311

Realistic Effective Interaction

two-body densities

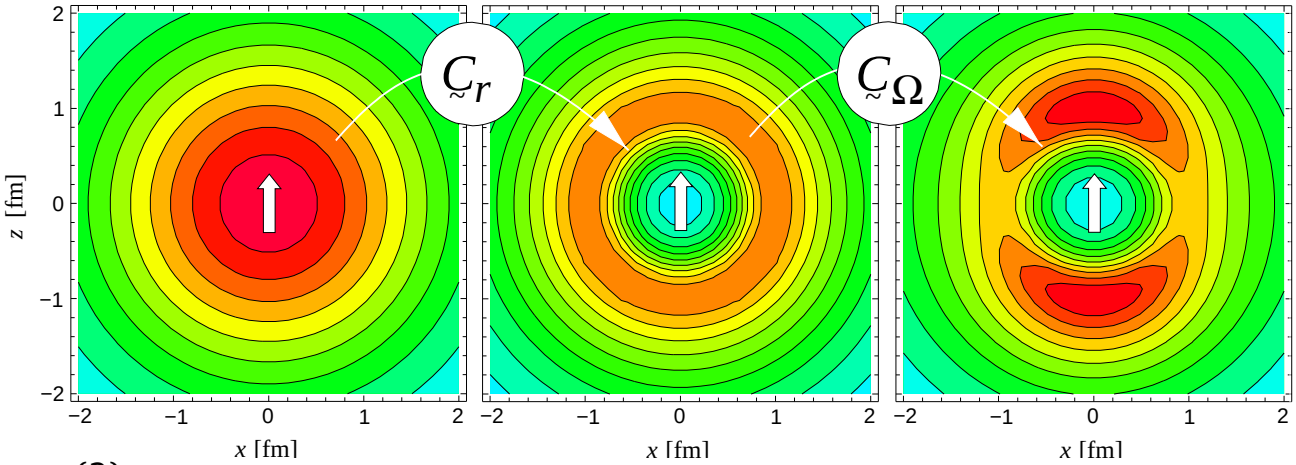

$\rho^{(2)}_{S,T}(\mathbf{r}_1 - \mathbf{r}_2) \quad S = 1, M_S = 1, T = 0$

central correlator C_r shifts density out of the repulsive core

tensor correlator C_Ω aligns density with spin orientation

both central and tensor correlations are essential for binding

energies

$0\hbar\omega$ Harmonic Oscillator

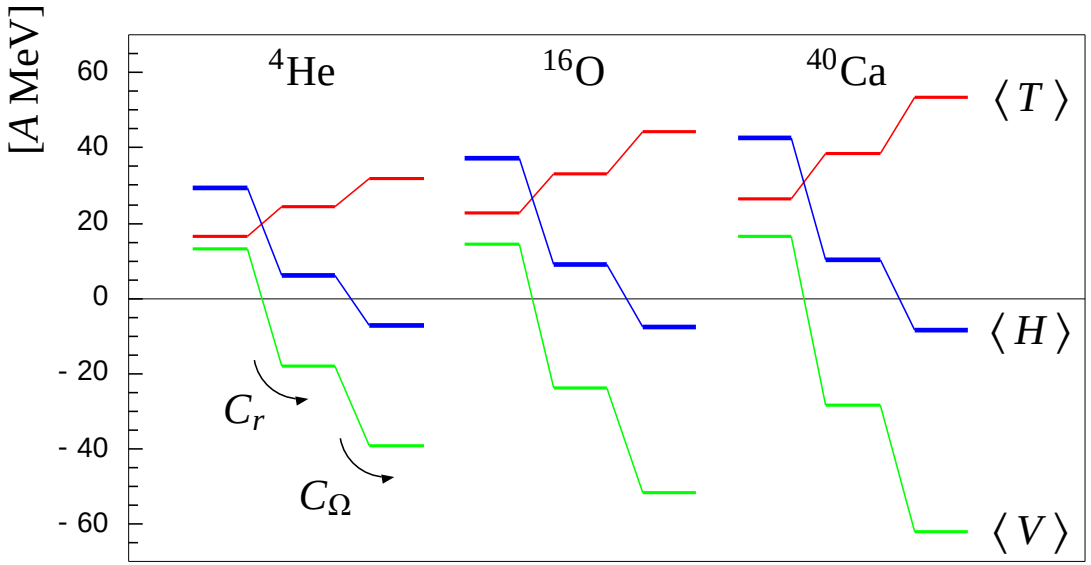

Neff and Feldmeier, Nucl. Phys. **A713** (2003) 311

Correlated Interaction in Momentum Space

$^3S_1$ bare

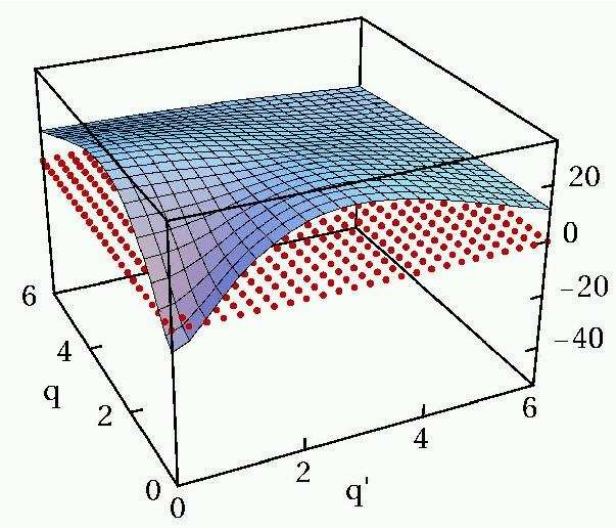

bare interaction has **strong off-diagonal** matrix elements connecting to high momenta

$^3S_1$ - $^3D_1$ bare

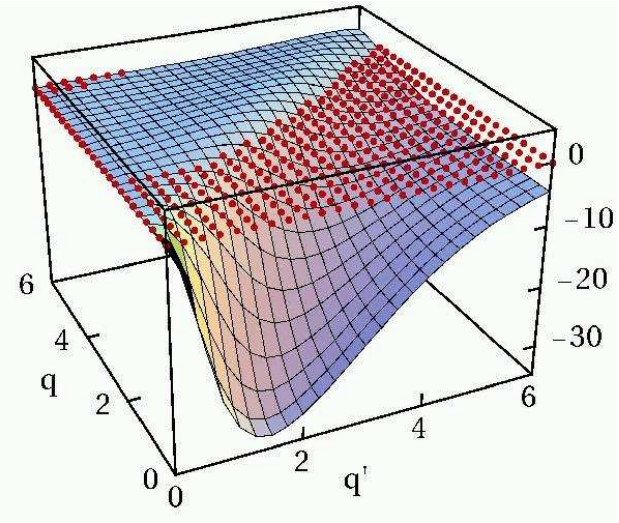

Roth, Hergert, Papakonstaninou, Neff, Feldmeier, Phys. Rev. C **72**, 034002 (2005)

Unitary Correlation Operator Method

Correlated Interaction in Momentum Space

$^3S_1$ bare

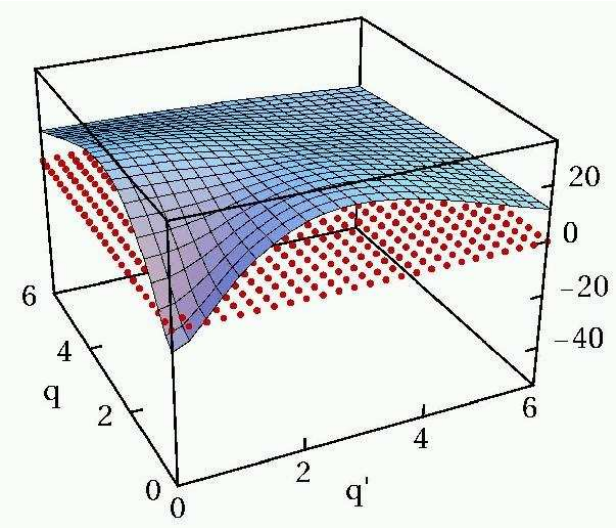

bare interaction has **strong off-diagonal** matrix elements connecting to high momenta

$^3S_1$ - $^3D_1$ bare

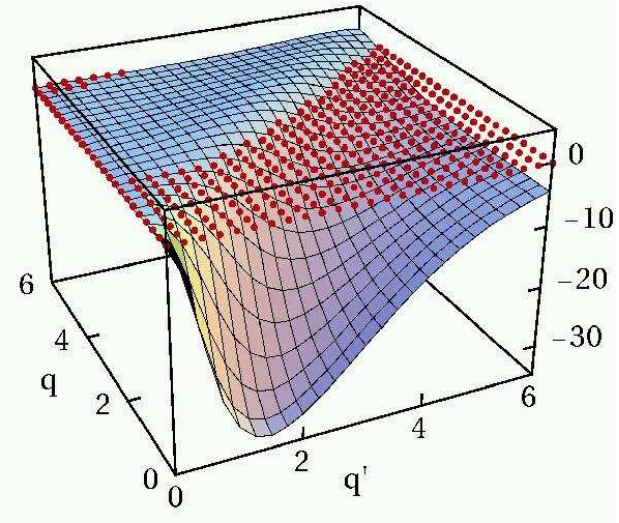

$^3S_1$ correlated

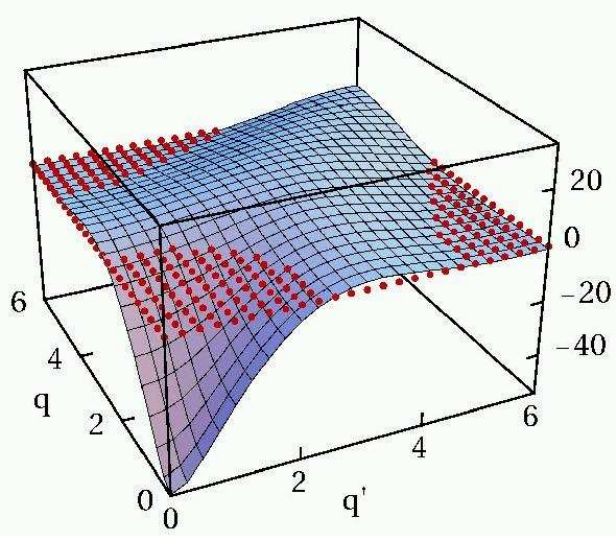

correlated interaction is **more attractive** at low momenta

$^3S_1$ - $^3D_1$ correlated

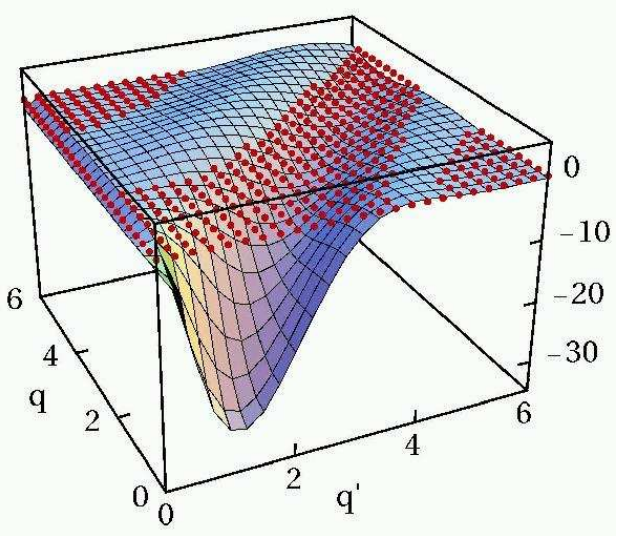

off-diagonal matrix elements connecting low- and high- momentum states are **strongly reduced**

Roth, Hergert, Papakonstaninou, Neff, Feldmeier, Phys. Rev. C **72**, 034002 (2005)

Unitary Correlation Operator Method

Correlated Interaction in Momentum Space

$^3S_1$ bare

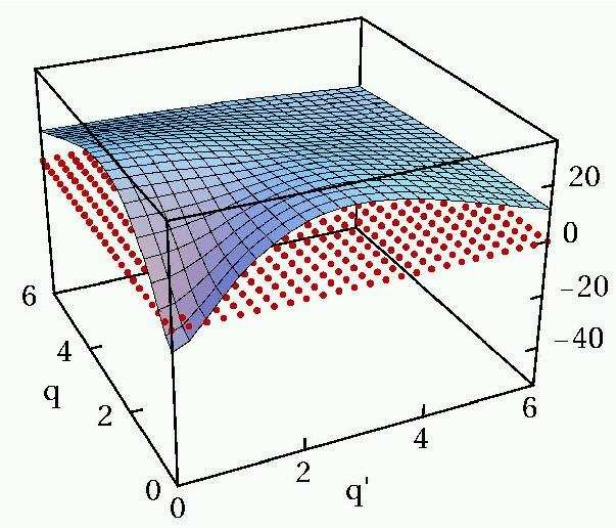

bare interaction has **strong off-diagonal** matrix elements connecting to high momenta

$^3S_1$ - $^3D_1$ bare

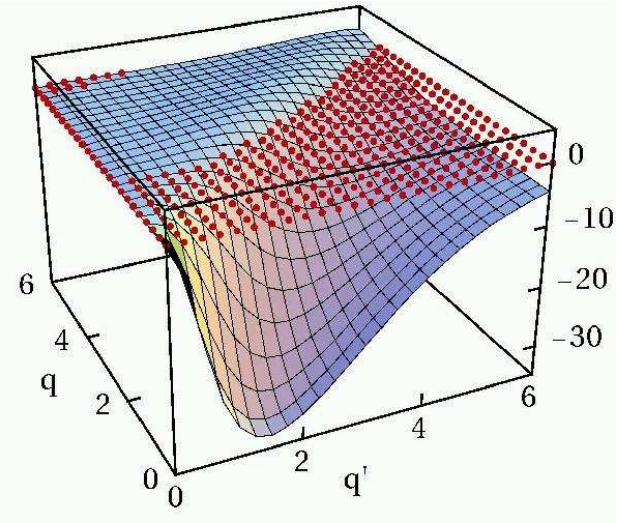

$^3S_1$ correlated

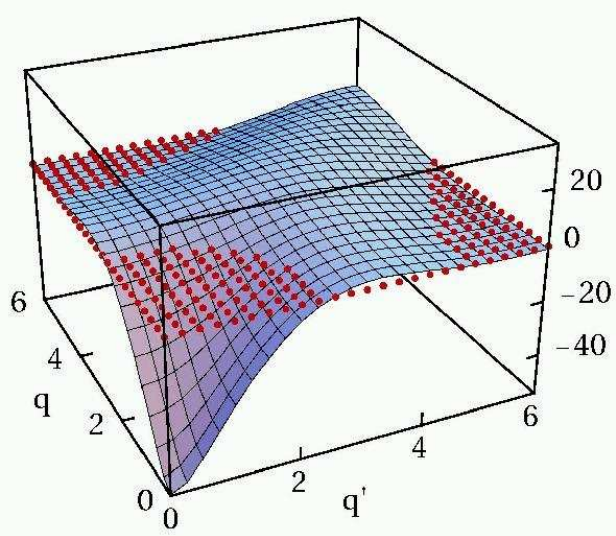

correlated interaction is **more attractive** at low momenta

$^3S_1$ - $^3D_1$ correlated

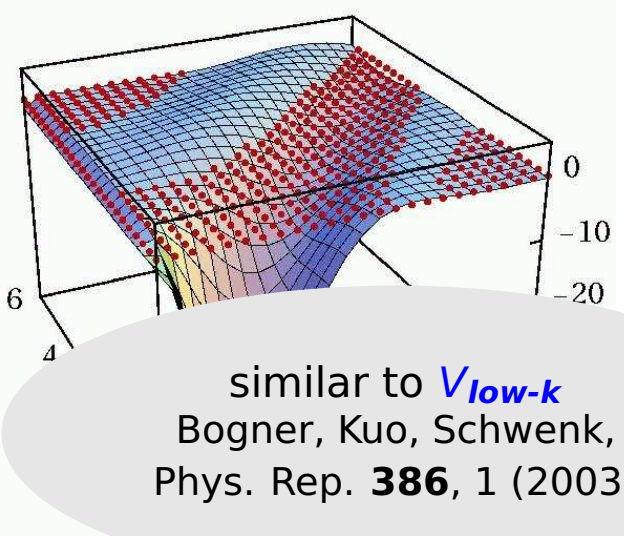

off-diagonal matrix elements connecting low- and high- momentum states are **strongly reduced**

similar to $V_{low\text{-}k}$
Bogner, Kuo, Schwenk, Phys. Rep. **386**, 1 (2003)

Roth, Hergert, Papakonstaninou, Neff, Feldmeier, Phys. Rev. C **72**, 034002 (2005)

Tjon Line and Three-body Contributions

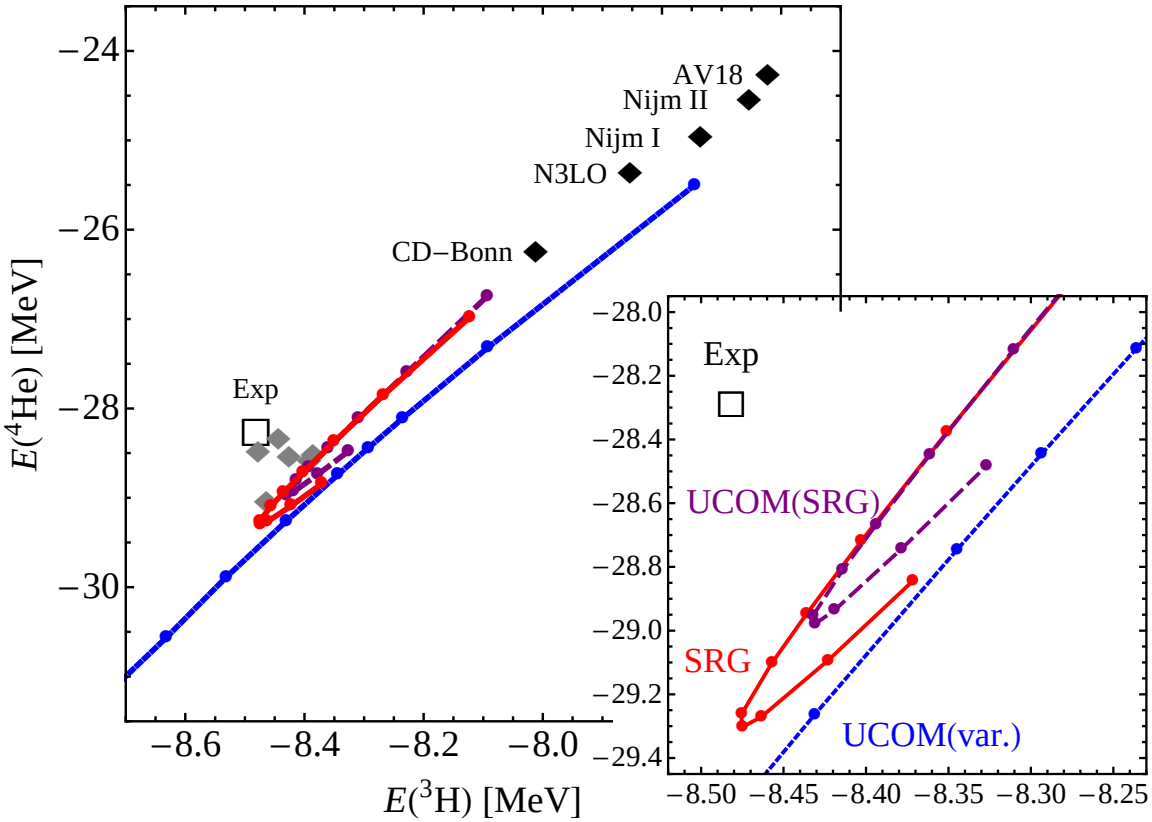

- choose tensor correlation range or SRG flow parameter α such that **need for three-body forces is minimized**

➨ **different perspective**: don't try to reproduce the results with the bare interaction but consider $\mathbf{V_{UCOM}}$ **as a realistic potential**

UCOM
NCFC ^{6}Li

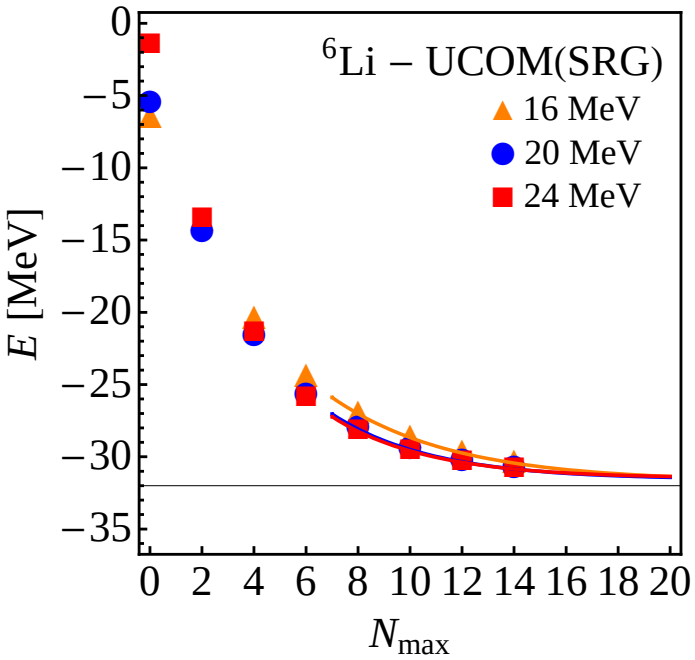

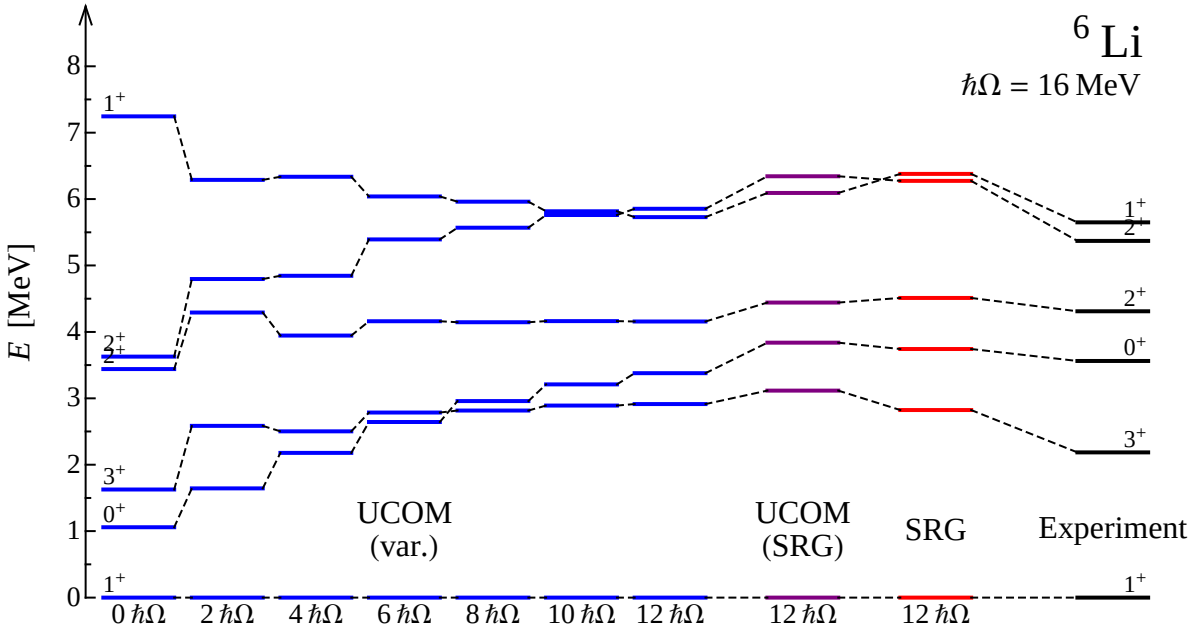

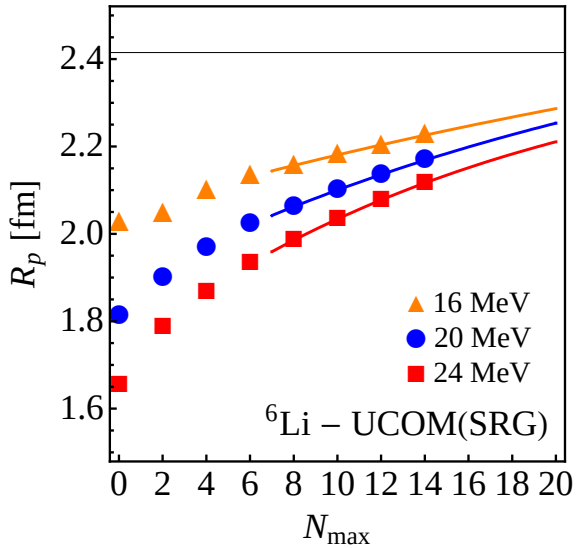

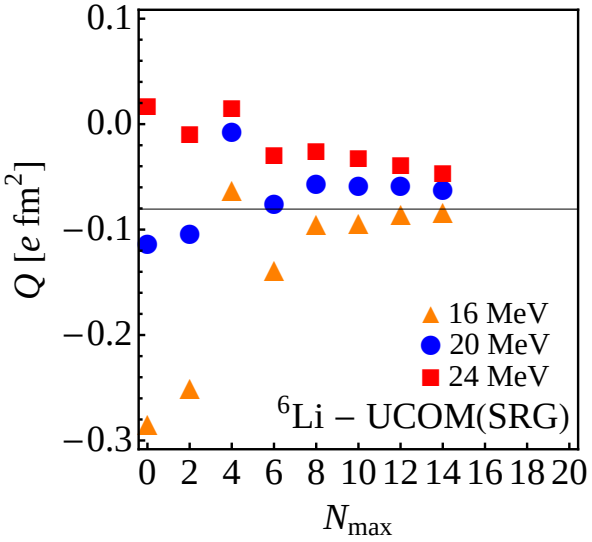

- Convergence dramatically improved compared to bare interaction
- Binding energy close to experiment
- Spectra with V_{UCOM} are of similar quality than with other modern NN forces

Roth, Neff, Feldmeier, arXiv:1003.3624

Hartree-Fock calculations

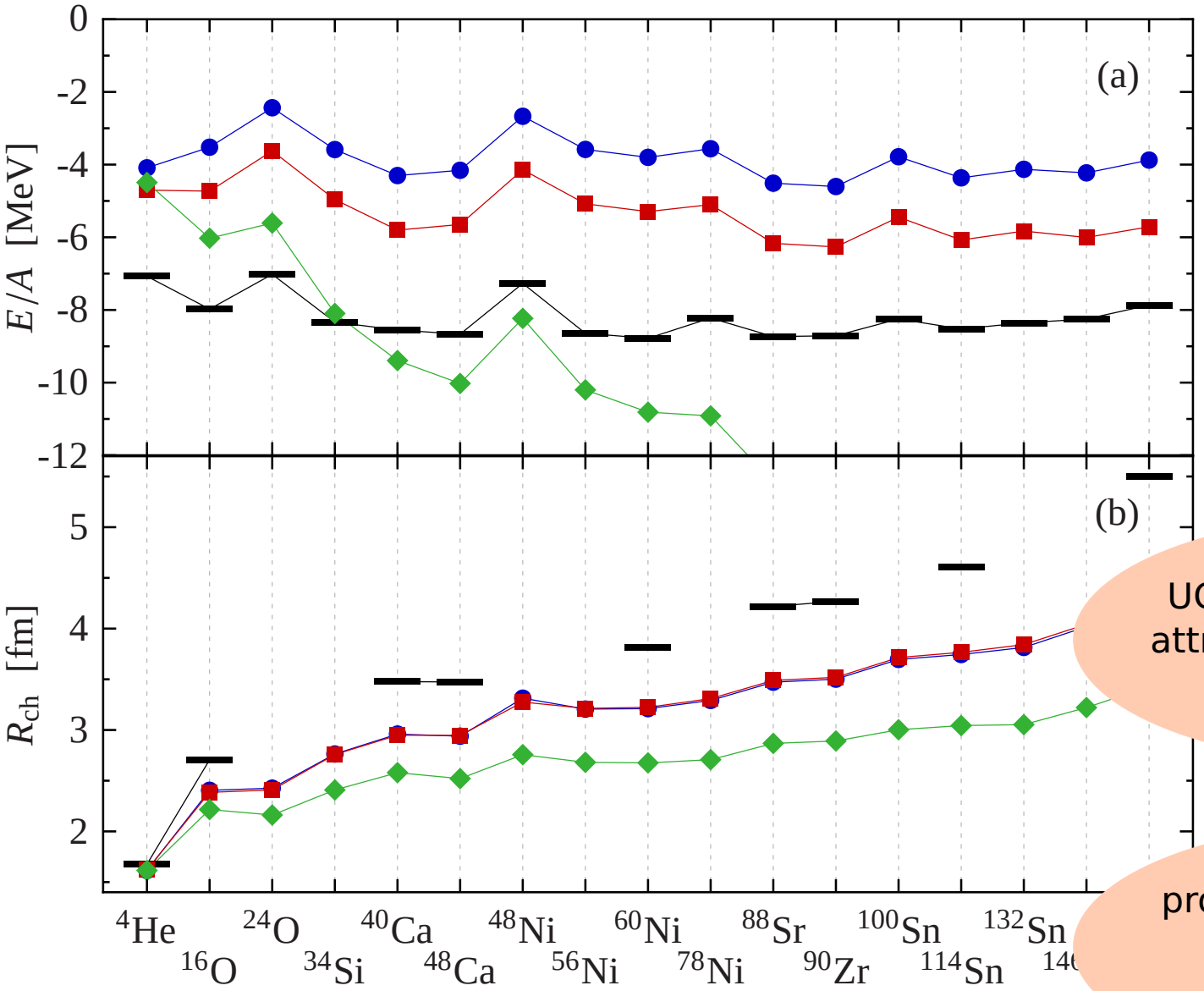

- UCOM(var.)
- UCOM(SRG)
- SRG

spherical Hartree-Fock in 12 $\hbar\omega$ harmonic oscillator basis

UCOM interaction is less attractive in higher partial waves

problems with saturation indicate need for **three-body forces**

Roth, Neff, Feldmeier, arXiv:1003.3624

Fermionic Molecular Dynamics

Motivation

FMD Wave Functions

Nucleon-Nucleon Interaction

Mean-Field Calculations

**Projection After Variation,
Variation After Projection
and Multiconfiguration**

Exotica: Special Challenges

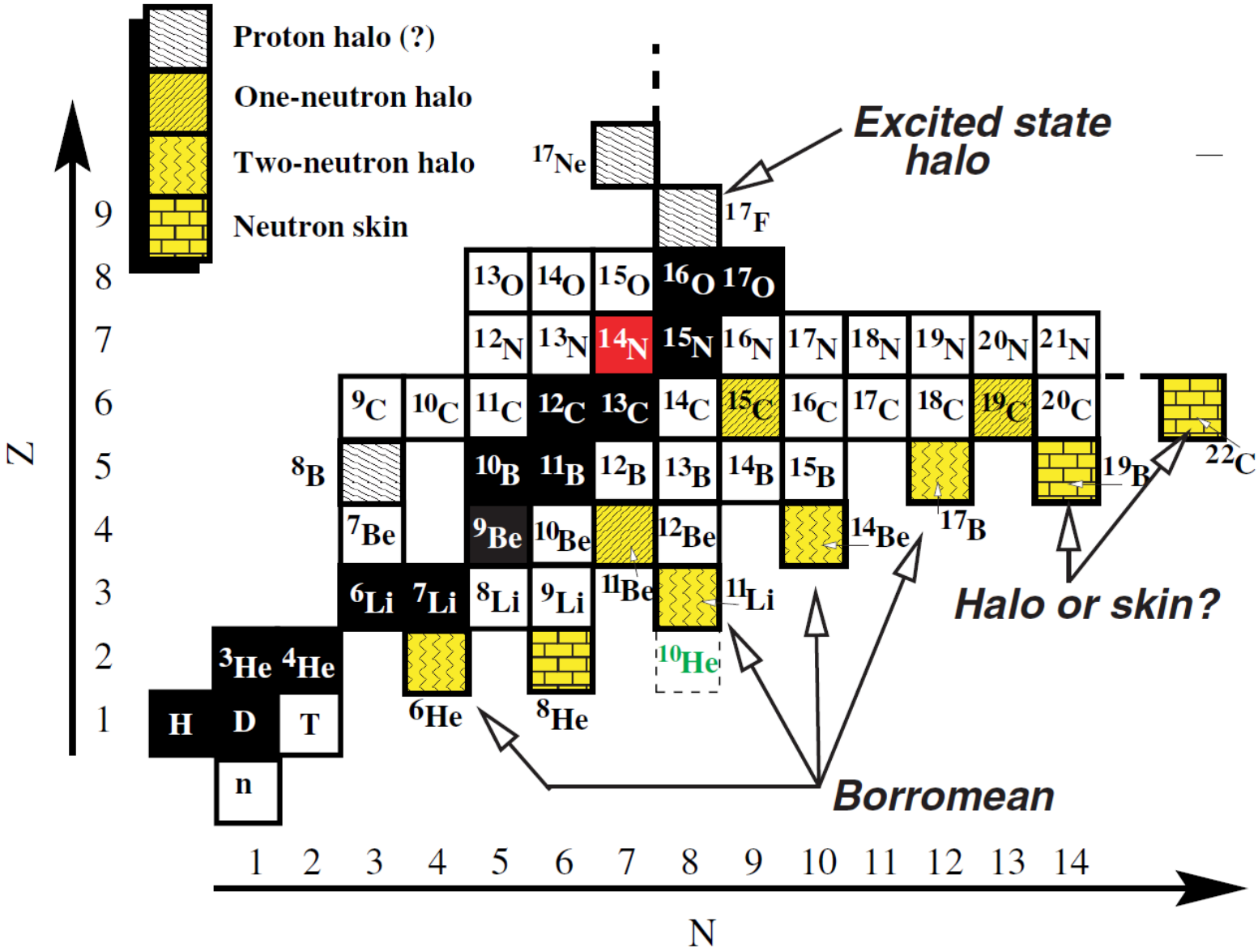

Al-Khalili, Nunes, J. Phys. G **29**, R89 (2003)

Fermionic Molecular Dynamics

Fermionic

Slater determinant

$$\left| Q \right\rangle = \underset{\sim}{\mathcal{A}} \left(\left| q_1 \right\rangle \otimes \cdots \otimes \left| q_A \right\rangle \right)$$

- antisymmetrized A-body state

Feldmeier, Schnack, Rev. Mod. Phys. **72** (2000) 655

Neff, Feldmeier, Nucl. Phys. **A738** (2004) 357

Fermionic Molecular Dynamics

Fermionic

Slater determinant

$$\left| Q \right\rangle = \underset{\sim}{\mathcal{A}} \left(\left| q_1 \right\rangle \otimes \cdots \otimes \left| q_A \right\rangle \right)$$

- antisymmetrized A-body state

Molecular

single-particle states

$$\left\langle \mathbf{x} \middle| q \right\rangle = \sum_i c_i \exp\left\{ -\frac{(\mathbf{x} - \mathbf{b}_i)^2}{2a_i} \right\} \otimes \left| \chi^{\uparrow}_i, \chi^{\downarrow}_i \right\rangle \otimes \left| \xi \right\rangle$$

- Gaussian wave-packets in phase-space (complex parameter $\mathbf{b}_i$ encodes mean position and mean momentum), spin is free, isospin is fixed
- width a_i is an independent variational parameter for each wave packet
- use one or two wave packets for each single particle state

Feldmeier, Schnack, Rev. Mod. Phys. **72** (2000) 655

Neff, Feldmeier, Nucl. Phys. **A738** (2004) 357

FMD

Fermionic Molecular Dynamics

Fermionic

Slater determinant

$$|Q\rangle = \mathcal{A}\Big(|q_1\rangle \otimes \cdots \otimes |q_A\rangle\Big)$$

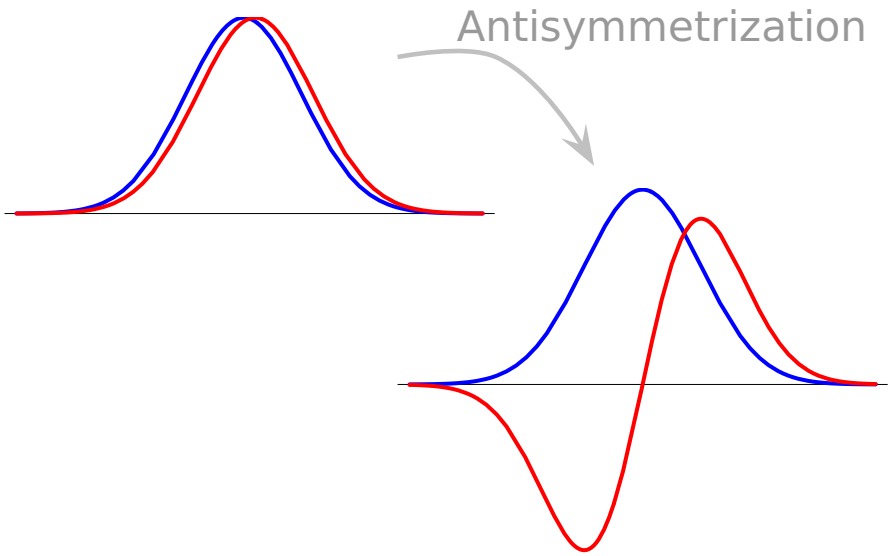

- antisymmetrized A-body state

Molecular

single-particle states

$$\langle \mathbf{x}|q\rangle = \sum_i c_i \exp\left\{-\frac{(\mathbf{x}-\mathbf{b}_i)^2}{2a_i}\right\} \otimes |\chi^{\uparrow}_i, \chi^{\downarrow}_i\rangle \otimes |\xi\rangle$$

- Gaussian wave-packets in phase-space (complex parameter $\mathbf{b}_i$ encodes mean position and mean momentum), spin is free, isospin is fixed
- width a_i is an independent variational parameter for each wave packet
- use one or two wave packets for each single particle state

Feldmeier, Schnack, Rev. Mod. Phys. **72** (2000) 655

Neff, Feldmeier, Nucl. Phys. **A738** (2004) 357

FMD

Fermionic Molecular Dynamics

Fermionic

Slater determinant

$$|Q\rangle = \mathcal{A}\Big(|q_1\rangle \otimes \cdots \otimes |q_A\rangle\Big)$$

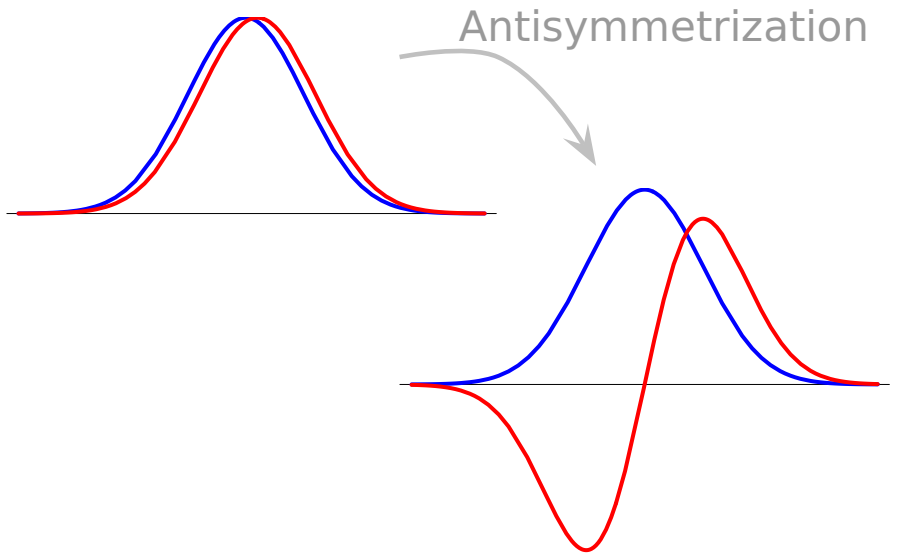

- antisymmetrized A-body state

Molecular

single-particle states

$$\langle \mathbf{x}|q\rangle = \sum_i c_i \exp\left\{-\frac{(\mathbf{x}-\mathbf{b}_i)^2}{2a_i}\right\} \otimes |\chi^{\uparrow}_i, \chi^{\downarrow}_i\rangle \otimes |\xi\rangle$$

- Gaussian wave-packets in phase-space (complex parameter $\mathbf{b}_i$ encodes mean position and mean momentum), spin is free, isospin is fixed
- width a_i is an independent variational parameter for each wave packet
- use one or two wave packets for each single particle st

see also
Antisymmetrized Molecular Dynamics
H. Horiuchi, Y. Kanada-En'yo

Feldmeier, Schnack, Rev. Mod. Phys. **72** (2000) 655

Neff, Feldmeier, Nucl. Phys. **A738** (2004) 357

Evaluation of Matrix Elements

- non-orthogonal basis, use inverse overlap matrix

One-Body Operators

$$\frac{\langle Q \left| \underset{\sim}{T}^{[1]} \right| Q \rangle}{\langle Q \left| Q \right. \rangle} = \sum_{k,l}^{A} \langle q_k \left| \underset{\sim}{T}^{[1]} \right| q_l \rangle \, o_{lk}$$

Two-Body Operators

$$\frac{\langle Q \left| \underset{\sim}{V}^{[2]} \right| Q \rangle}{\langle Q \left| Q \right. \rangle} = \frac{1}{2} \sum_{k,l,m,n}^{A} \langle q_k, q_l \left| \underset{\sim}{V}^{[2]} \right| q_m, q_n \rangle \, (o_{mk} o_{nl} - o_{ml} o_{nk})$$

$$o = n^{-1} = \left(\langle q_i \left| q_j \right. \rangle \right)^{-1}$$

Interaction Matrix Elements

(One-body) Kinetic Energy

$$\langle q_k \left| \underset{\sim}{T} \right| q_l \rangle = \langle a_k \mathbf{b}_k \left| \underset{\sim}{T} \right| a_l \mathbf{b}_l \rangle \langle \chi_k | \chi_l \rangle \langle \xi_k | \xi_l \rangle$$

$$\langle a_k \mathbf{b}_k \left| \underset{\sim}{T} \right| a_l \mathbf{b}_l \rangle = \frac{1}{2m} \left(\frac{3}{a_k^\star + a_l} - \frac{(\mathbf{b}_k^\star - \mathbf{b}_l)^2}{(a_k^\star + a_l)^2} \right) R_{kl}$$

(Two-body) Potential

- fit radial dependencies by (a sum of) Gaussians

$$G(\mathbf{x}_1 - \mathbf{x}_2) = \exp\left\{ -\frac{(\mathbf{x}_1 - \mathbf{x}_2)^2}{2\kappa} \right\}$$

- Gaussian integrals

$$\langle a_k \mathbf{b}_k, a_l \mathbf{b}_l \left| \underset{\sim}{G} \right| a_m \mathbf{b}_m, a_n \mathbf{b}_n \rangle = R_{km} R_{ln} \left(\frac{\kappa}{\alpha_{klmn} + \kappa} \right)^{3/2} \exp\left\{ -\frac{\boldsymbol{\rho}_{klmn}^2}{2(\alpha_{klmn} + \kappa)} \right\}$$

- analytical formulas for matrix elements

$$\alpha_{klmn} = \frac{a_k{}^\star a_m}{a_k{}^\star + a_m} + \frac{a_l{}^\star a_n}{a_l{}^\star + a_n}$$

$$\boldsymbol{\rho}_{klmn} = \frac{a_m \mathbf{b}_k{}^\star + a_k{}^\star \mathbf{b}_m}{a_k{}^\star + a_m} - \frac{a_n \mathbf{b}_l{}^\star + a_l{}^\star \mathbf{b}}{a_l{}^\star + a_n}$$

$$R_{km} = \langle a_k \mathbf{b}_k \left| a_m \mathbf{b}_m \right. \rangle$$

Effective interaction based on V_{UCOM}

Effective two-body interaction

- FMD model space can't describe correlations induced by residual medium-long ranged tensor forces

➨ use **long ranged tensor correlator – "low cutoff"** to partly account for that

- no three-body forces, missing spin-orbit strength, radii tend to be too small

➨ add phenomenological two-body correction term with a **momentum-dependend** central and (isospin-dependend) **spin-orbit** part (about 15% contribution to potential)

➨ fit correction term to binding energies and radii of "closed-shell" nuclei (^{4}He, ^{16}O, ^{40}Cα), (^{24}O, ^{34}Si, ^{48}Cα)

➨ **Outlook:**
use **three-body** or **density dependent two-body force** instead of two-body correction term

Mean-Field Calculations

Minimization

- minimize Hamiltonian expectation value with respect to all single-particle parameters q_k

$$\min_{\{q_k\}} \frac{\langle Q \left| \underset{\sim}{H} - \underset{\sim}{T}_{cm} \right| Q \rangle}{\langle Q \left| Q \right\rangle}$$

- this is a Hartree-Fock calculation in our particular single-particle basis
- the mean-field may break the symmetries of the Hamiltonian

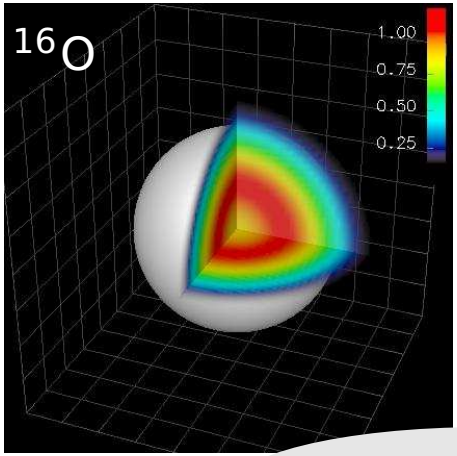

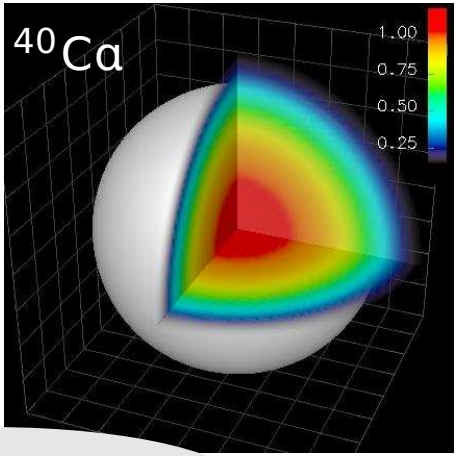

spherical nuclei

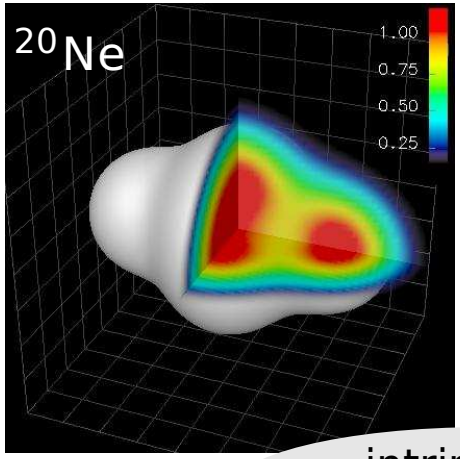

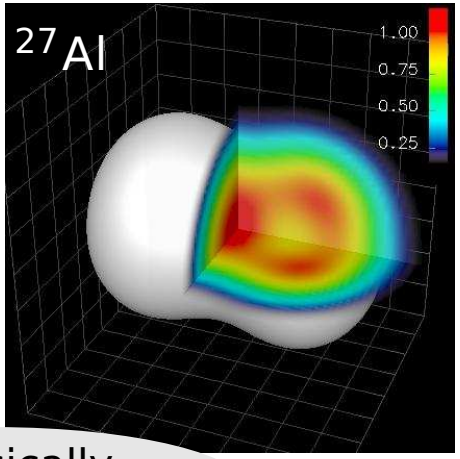

intrinsically deformed nuclei

PAV, VAP and Multiconfiguration

Projection After Variation (PAV)

- mean-field may break symmetries of Hamiltonian
- restore inversion, translational and rotational symmetry by projection on parity, linear and angular momentum

$$\underset{\sim}{P}^{\pi} = \frac{1}{2}(1 + \pi \underset{\sim}{\Pi})$$

$$\underset{\sim}{P}^{J}_{MK} = \frac{2J+1}{8\pi^2} \int \mathrm{d}^3\Omega \, {D^{J}_{MK}}^{\star}(\Omega) \, \underset{\sim}{R}(\Omega)$$

$$\underset{\sim}{P}^{\mathbf{P}} = \frac{1}{(2\pi)^3} \int \mathrm{d}^3X \; \exp\{-i(\underset{\sim}{\mathbf{P}} - \mathbf{P})\cdot\mathbf{X}\}$$

PAV, VAP and Multiconfiguration

Projection After Variation (PAV)

$$\underset{\sim}{P}^{\pi} = \frac{1}{2}(1 + \pi \underset{\sim}{\Pi})$$

- mean-field may break symmetries of Hamiltonian
- restore inversion, translational and rotational symmetry by projection on parity, linear and angular momentum

$$\underset{\sim}{P}^{J}_{MK} = \frac{2J+1}{8\pi^2} \int \mathrm{d}^3\Omega \, D^{J}_{MK}{}^{\star}(\Omega) \, \underset{\sim}{R}(\Omega)$$

Variation After Projection (VAP)

$$\underset{\sim}{P}^{\mathbf{P}} = \frac{1}{(2\pi)^3} \int \mathrm{d}^3X \, \exp\{-i(\underset{\sim}{\mathbf{P}} - \mathbf{P})\cdot\mathbf{X}\}$$

- effect of projection can be large
- full Variation after Angular Momentum and Parity Projection (VAP) for light nuclei
- perform VAP in GCM sense by applying **constraints** on radius, dipole moment, quadrupole moment or octupole moment and minimizing the energy in the projected energy surface for heavier nuclei

PAV, VAP and Multiconfiguration

Projection After Variation (PAV)

$$\underset{\sim}{P}^{\pi} = \frac{1}{2}(1 + \pi \underset{\sim}{\Pi})$$

- mean-field may break symmetries of Hamiltonian
- restore inversion, translational and rotational symmetry by projection on parity, linear and angular momentum

$$\underset{\sim}{P}^{J}_{MK} = \frac{2J+1}{8\pi^2} \int \mathrm{d}^3\Omega \, D^{J}_{MK}{}^{\star}(\Omega) \, \underset{\sim}{R}(\Omega)$$

Variation After Projection (VAP)

$$\underset{\sim}{P}^{\mathbf{P}} = \frac{1}{(2\pi)^3} \int \mathrm{d}^3X \, \exp\{-i(\underset{\sim}{\mathbf{P}} - \mathbf{P})\cdot\mathbf{X}\}$$

- effect of projection can be large
- full Variation after Angular Momentum and Parity Projection (VAP) for light nuclei
- perform VAP in GCM sense by applying **constraints** on radius, dipole moment, quadrupole moment or octupole moment and minimizing the energy in the projected energy surface for heavier nuclei

Multiconfiguration Calculations

- **diagonalize** Hamiltonian in a set of projected intrinsic states

$$\left\{ \left| Q^{(\alpha)} \right\rangle, \quad \alpha = 1, \ldots, N \right\}$$

$$\sum_{K'b} \left\langle Q^{(a)} \right| \underset{\sim}{H} \underset{\sim}{P}^{J^{\pi}}_{KK'} \underset{\sim}{P}^{\mathbf{P}=0} \left| Q^{(b)} \right\rangle \cdot c^{\alpha}_{K'b} =$$

$$E^{J^{\pi}\alpha} \sum_{K'b} \left\langle Q^{(a)} \right| \underset{\sim}{P}^{J^{\pi}}_{KK'} \underset{\sim}{P}^{\mathbf{P}=0} \left| Q^{(b)} \right\rangle \cdot c^{\alpha}_{K'b}$$

Beryllium Isotopes

Results still preliminary !

Questions

- α**-clustering, halos in** ^{11}Be **and** ^{14}Be**,** $N = 8$ **shell closure ?**

Calculation

- **FMD wave functions with two Gaussians per sp-state**
- **mean field, variation after projection, variation after multiconfiguration mixing**
- **VAP and multiconfiguration-VAP configurations with mean proton distance as generator coordinate**

Observables

- **energies**
- **charge and matter radii, electromagnetic transitions**

Beryllium Isotopes

Mean field

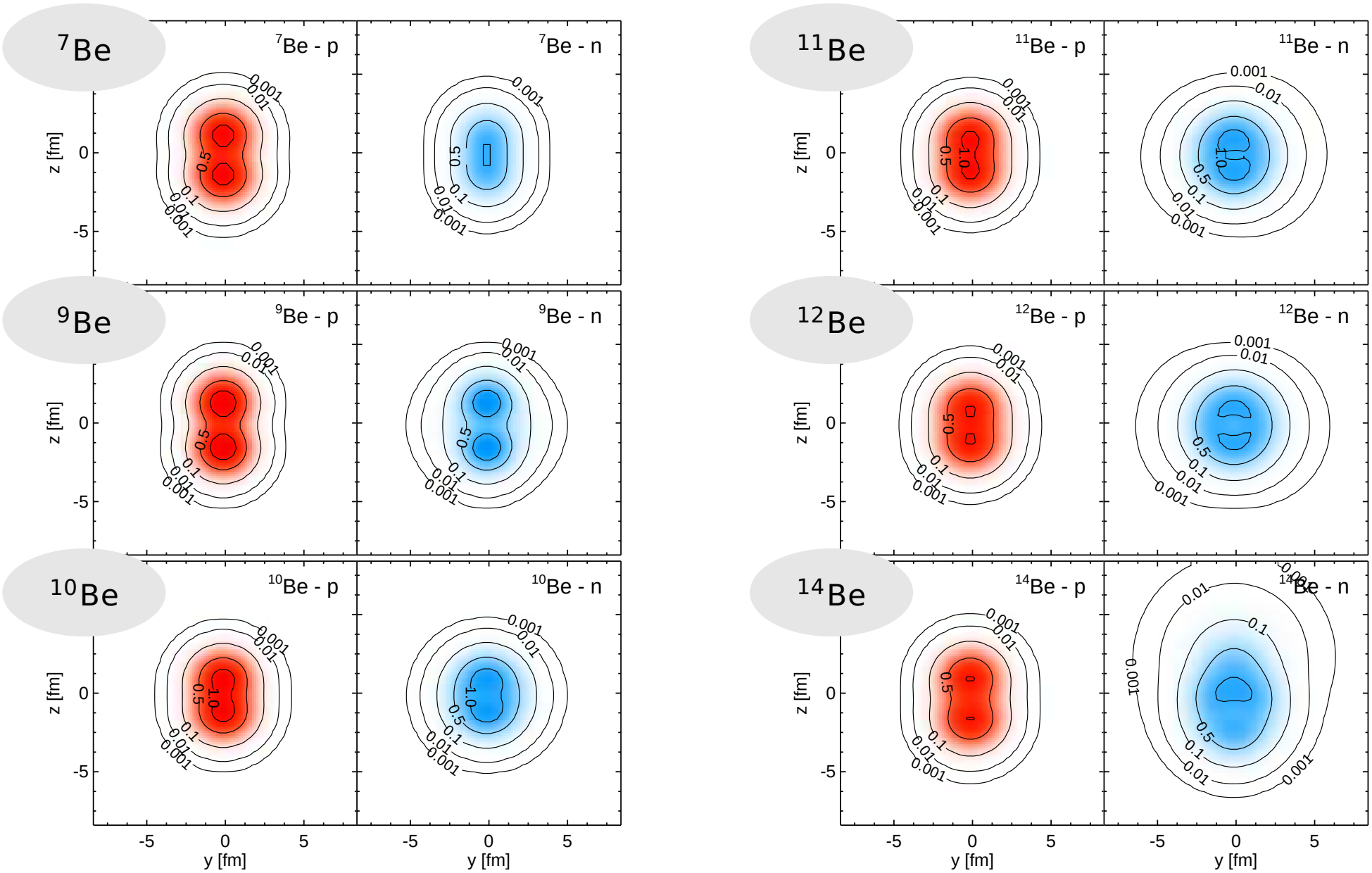

Variation after Projection

- create configurations by variation after parity and angular momentum projection

➨ large gain in binding energy compared to mean-field result

➨ intrinsic states show pronounced cluster structure. Parameters of ^{4}He and ^{3}He clusters are close to those of the free clusters

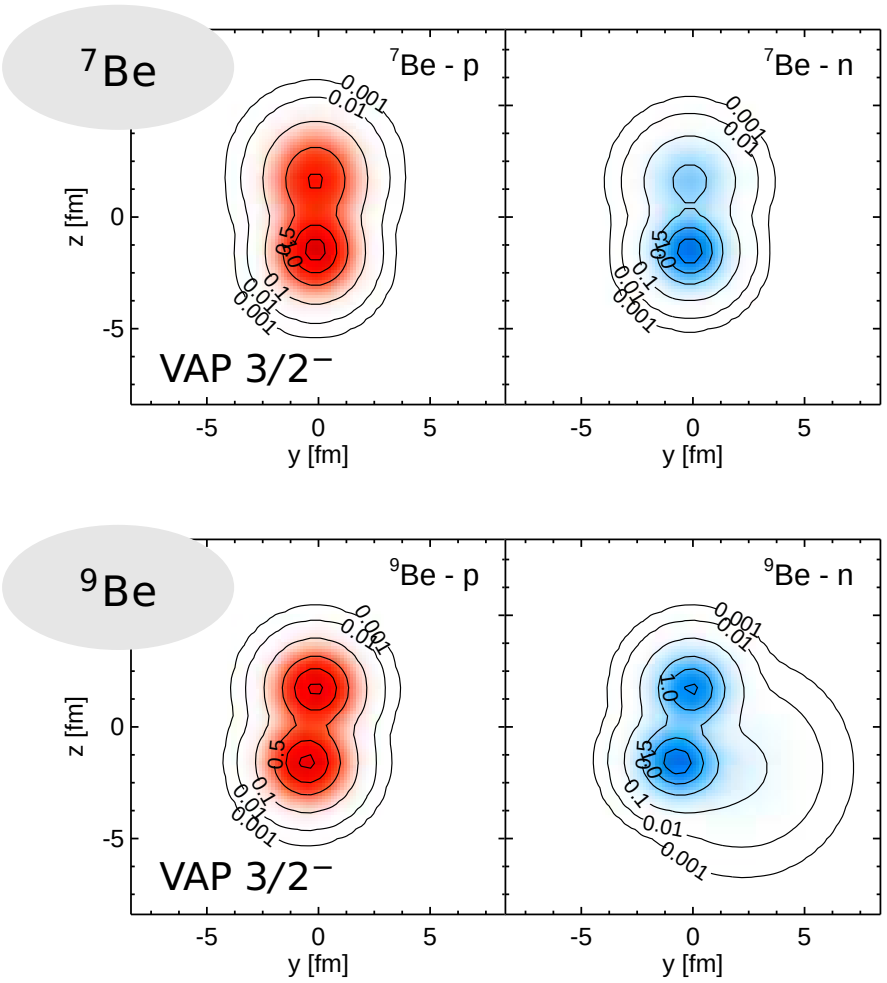

Variation after Projection

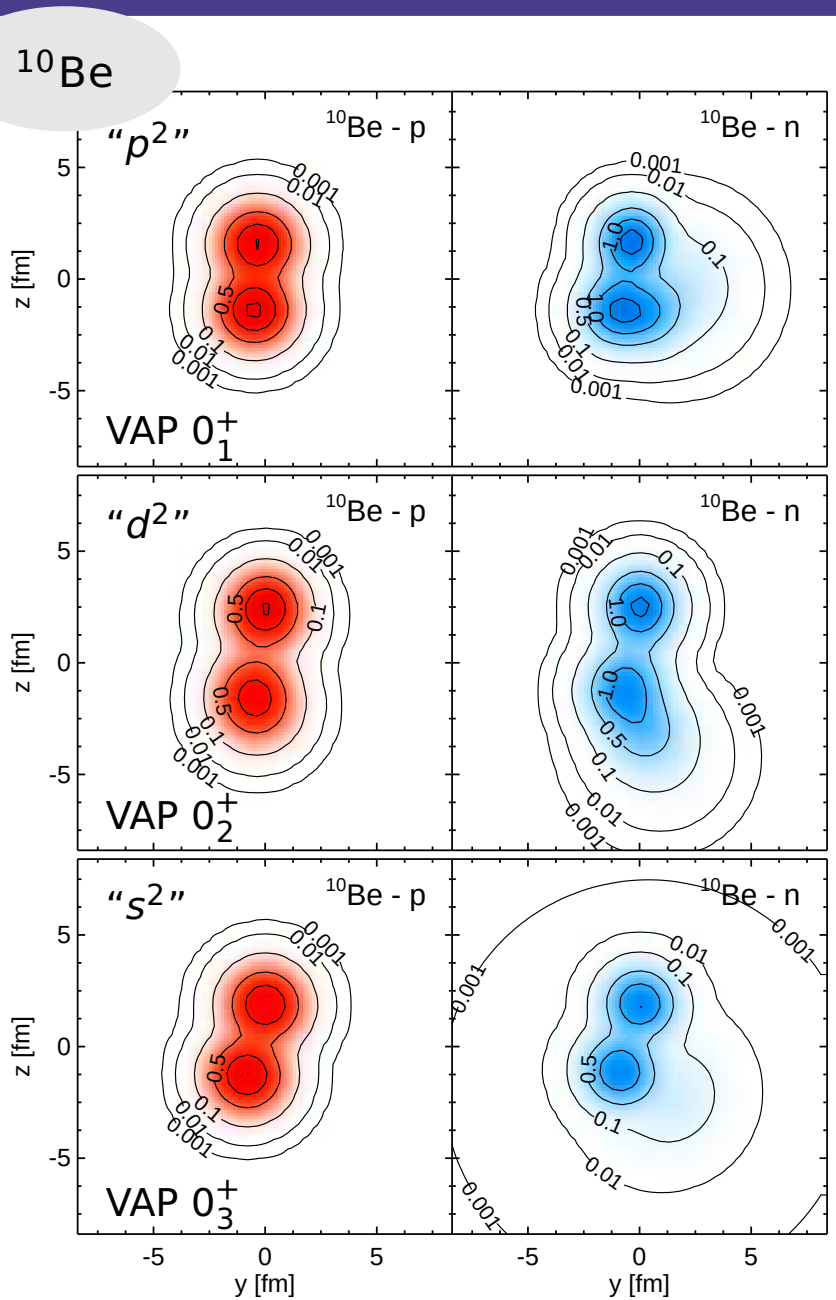

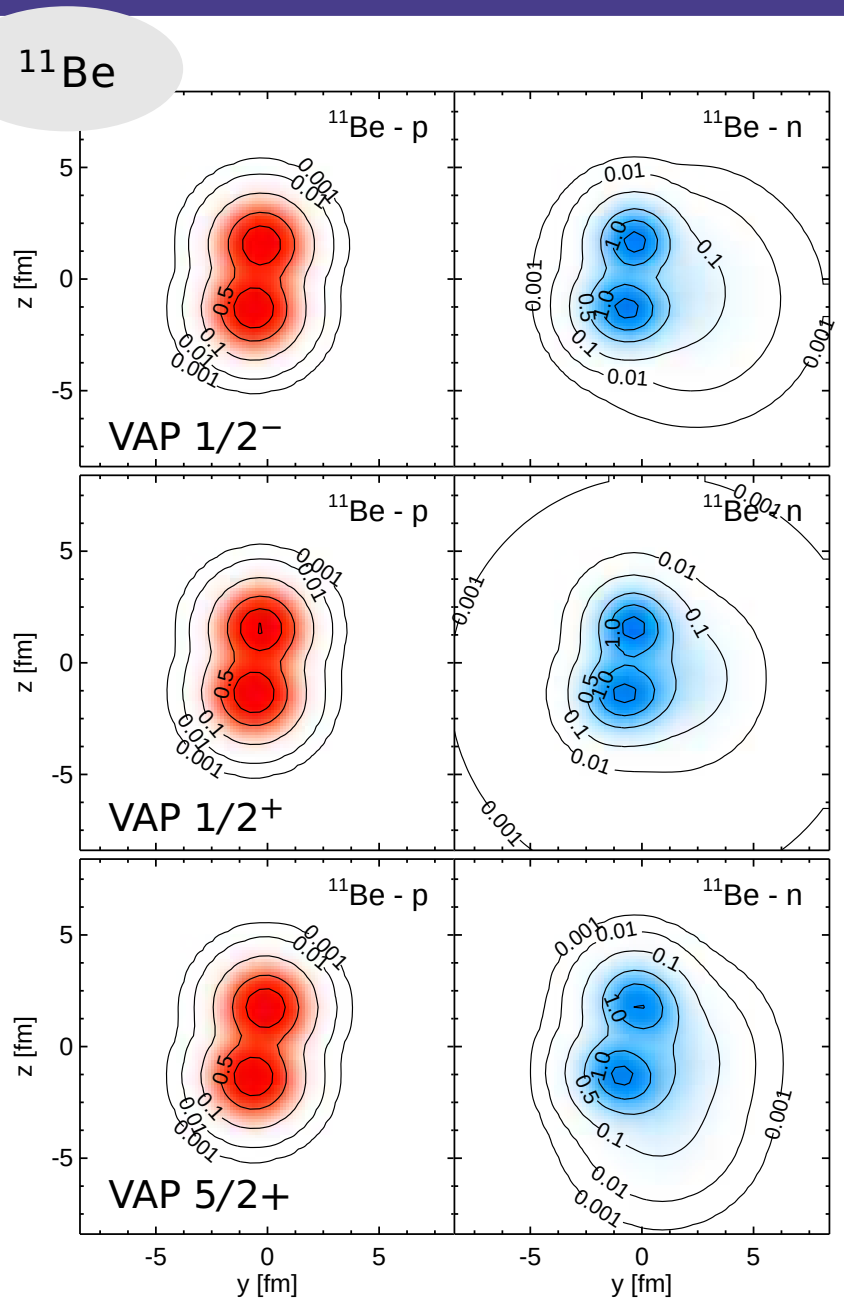

Variation after Projection

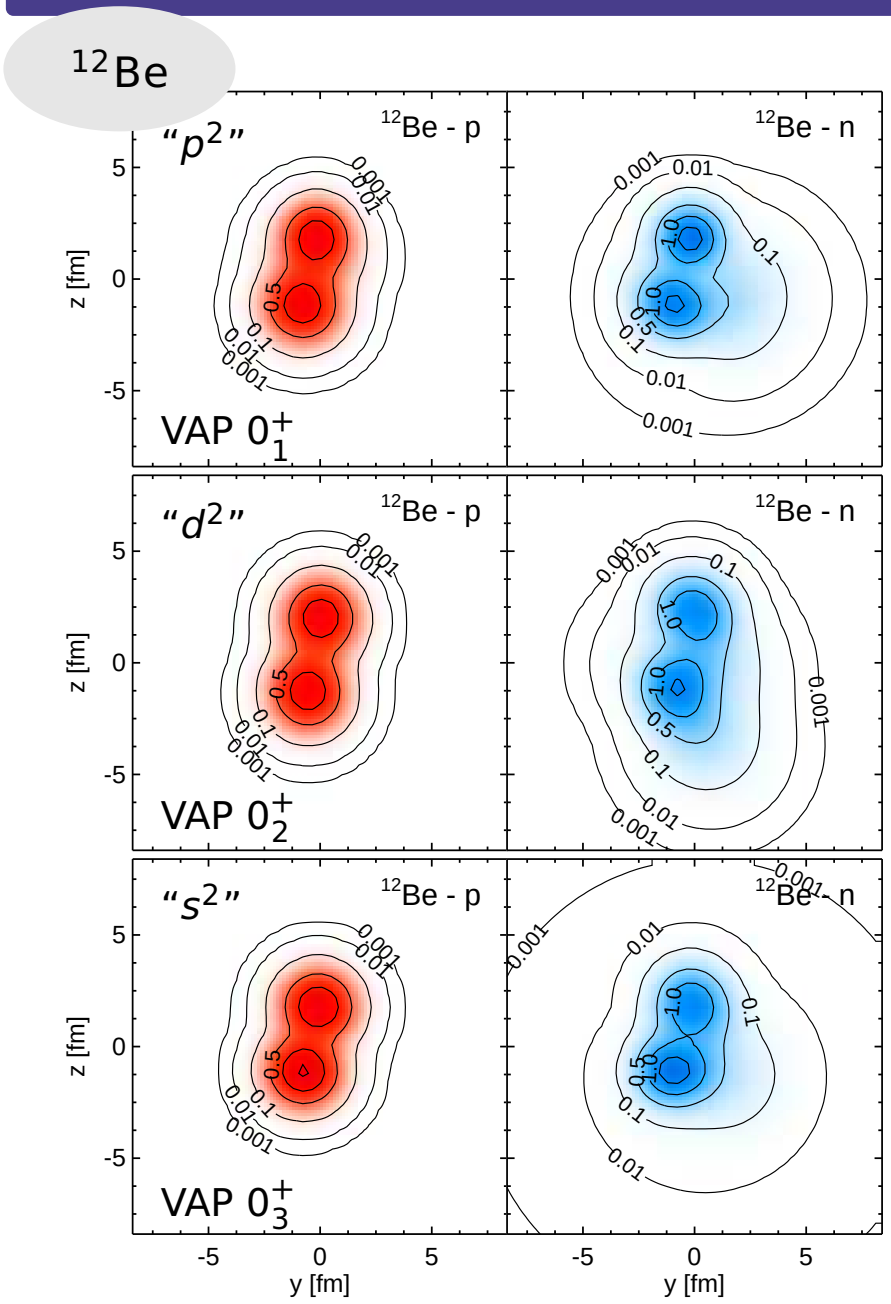

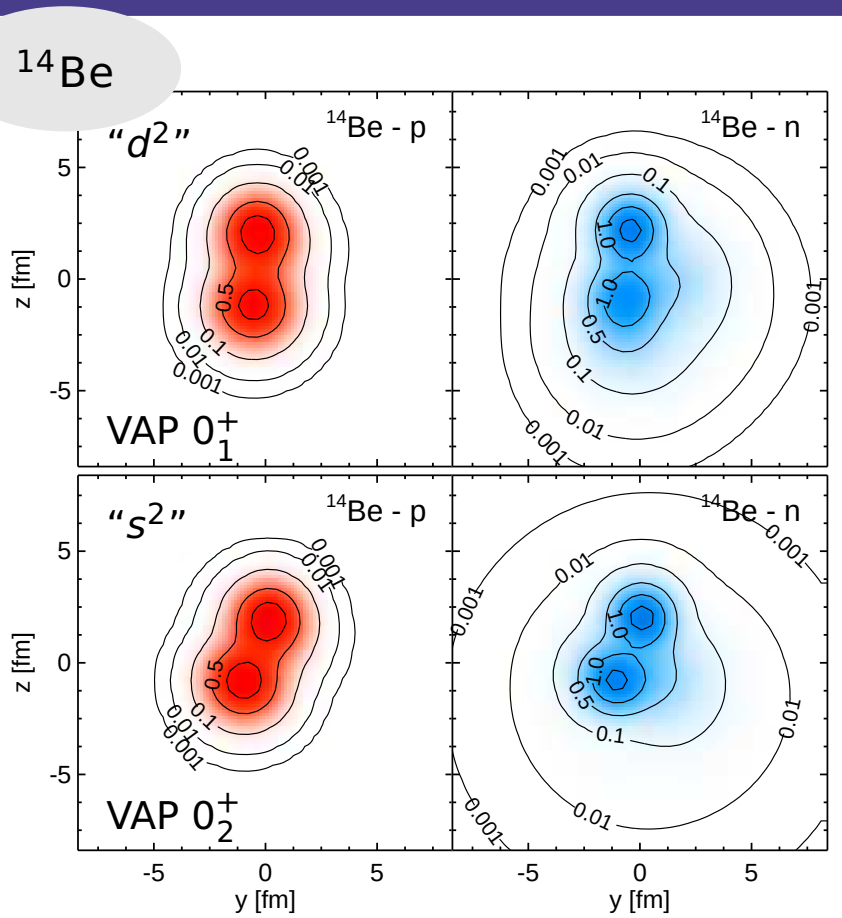

Mean proton distance as generator coordinate

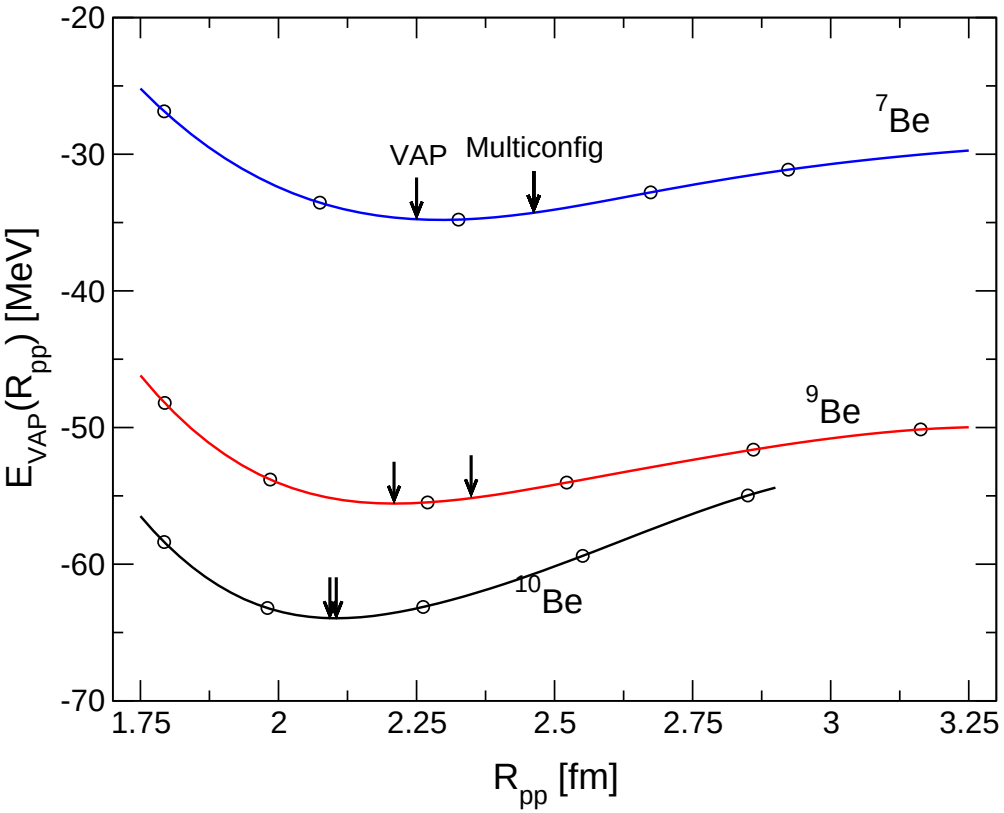

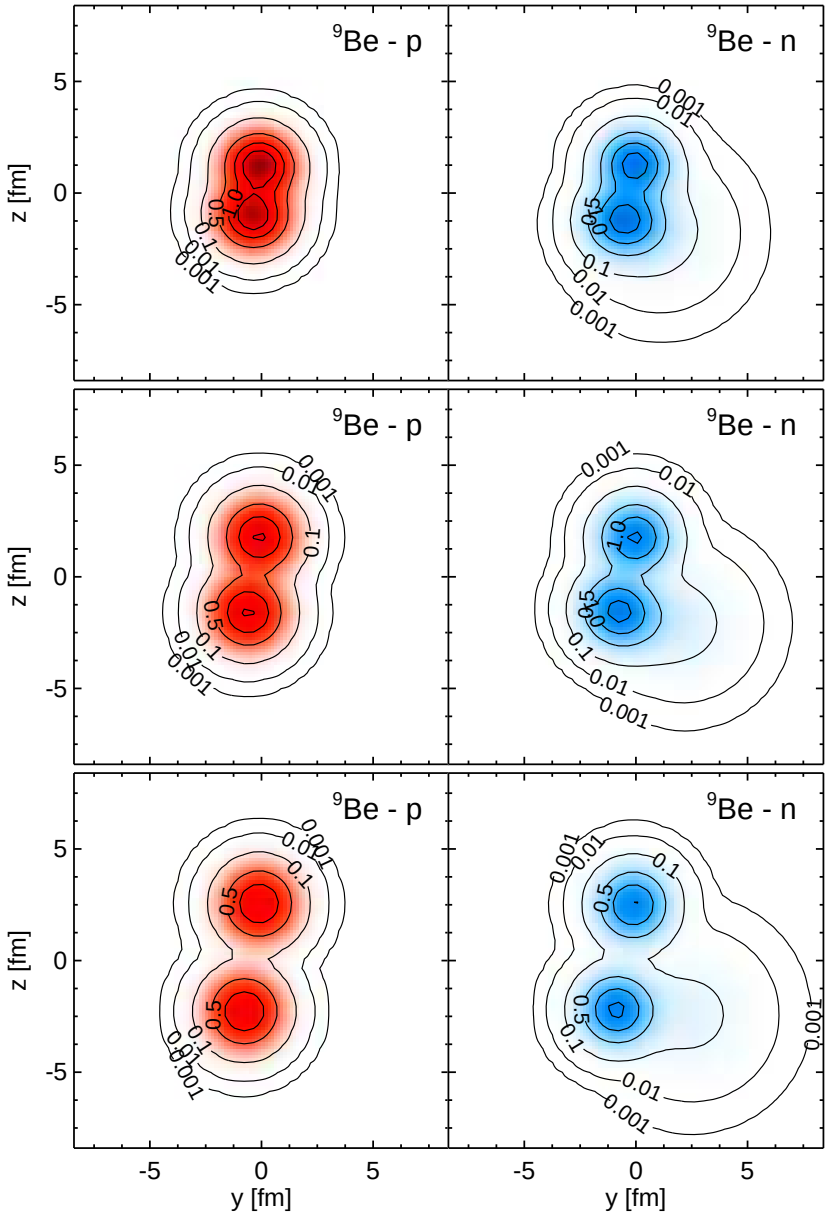

Mean proton distance

$$R_{pp}^2 = \frac{1}{Z^2}\langle \sum_{i<j}^{\text{protons}} (\mathbf{r}_i - \mathbf{r}_j)^2 \rangle$$

R_{pp} as a measure of
α-cluster distance

Mean proton distance as generator coordinate

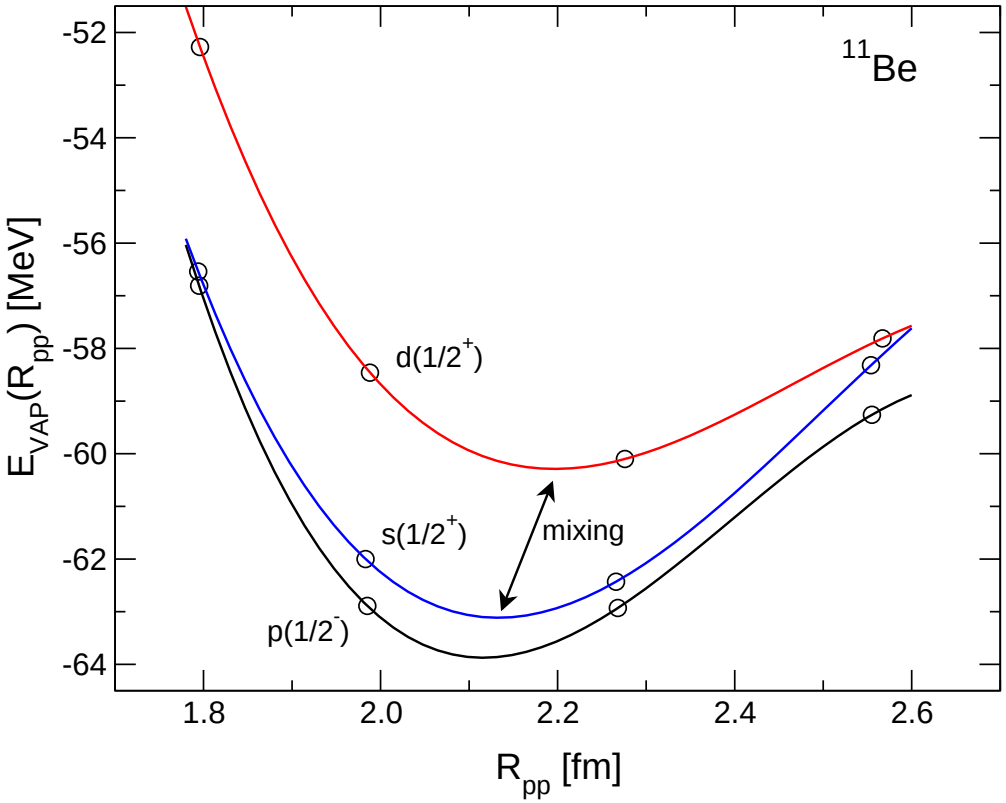

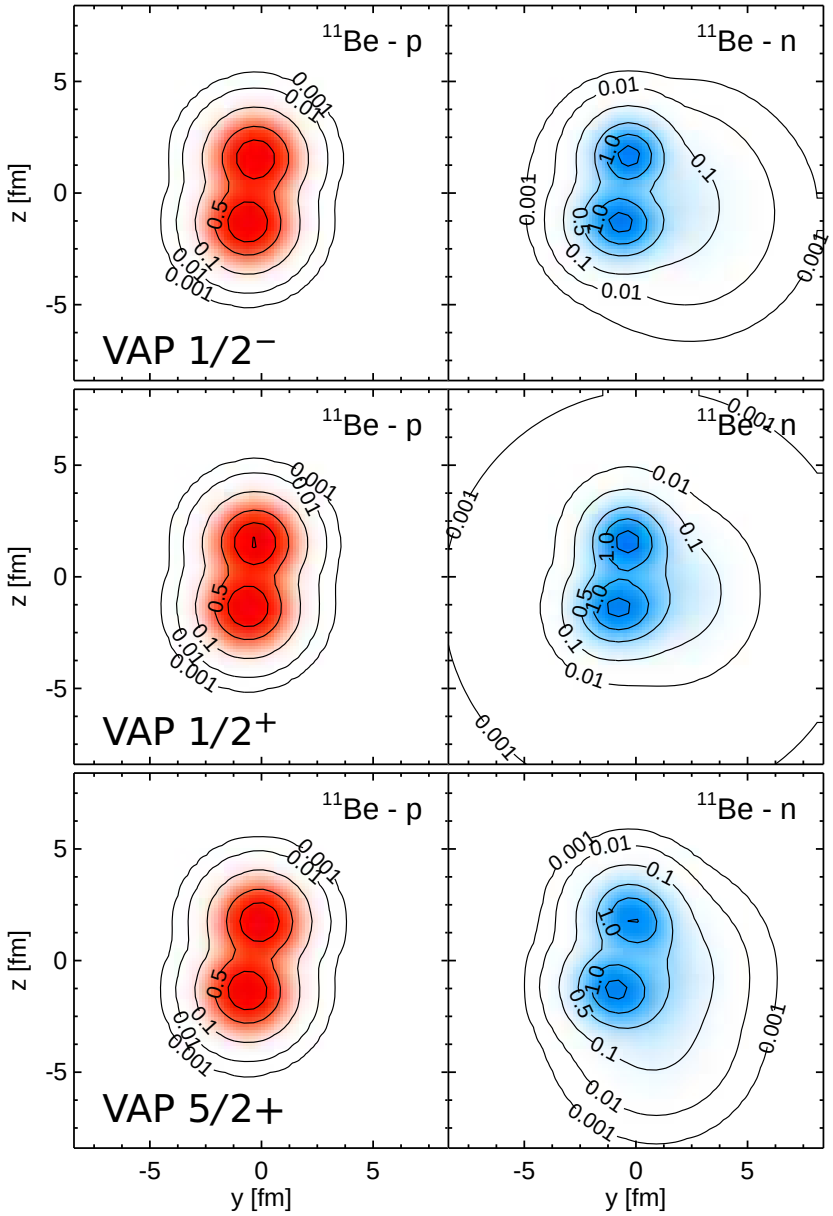

^{11}Be – "*p*", "*s*" and "*d*"-configurations

- "*s*"- and "*d*"-configurations will mix in 1/2$^+$ state
- energy surfaces for "*p*" and "*s*" similar to those in ^{10}Be
- "*d*" surface has minimum at larger cluster distance → *d*-configuration has a polarized ^{10}Be core

Binding energies

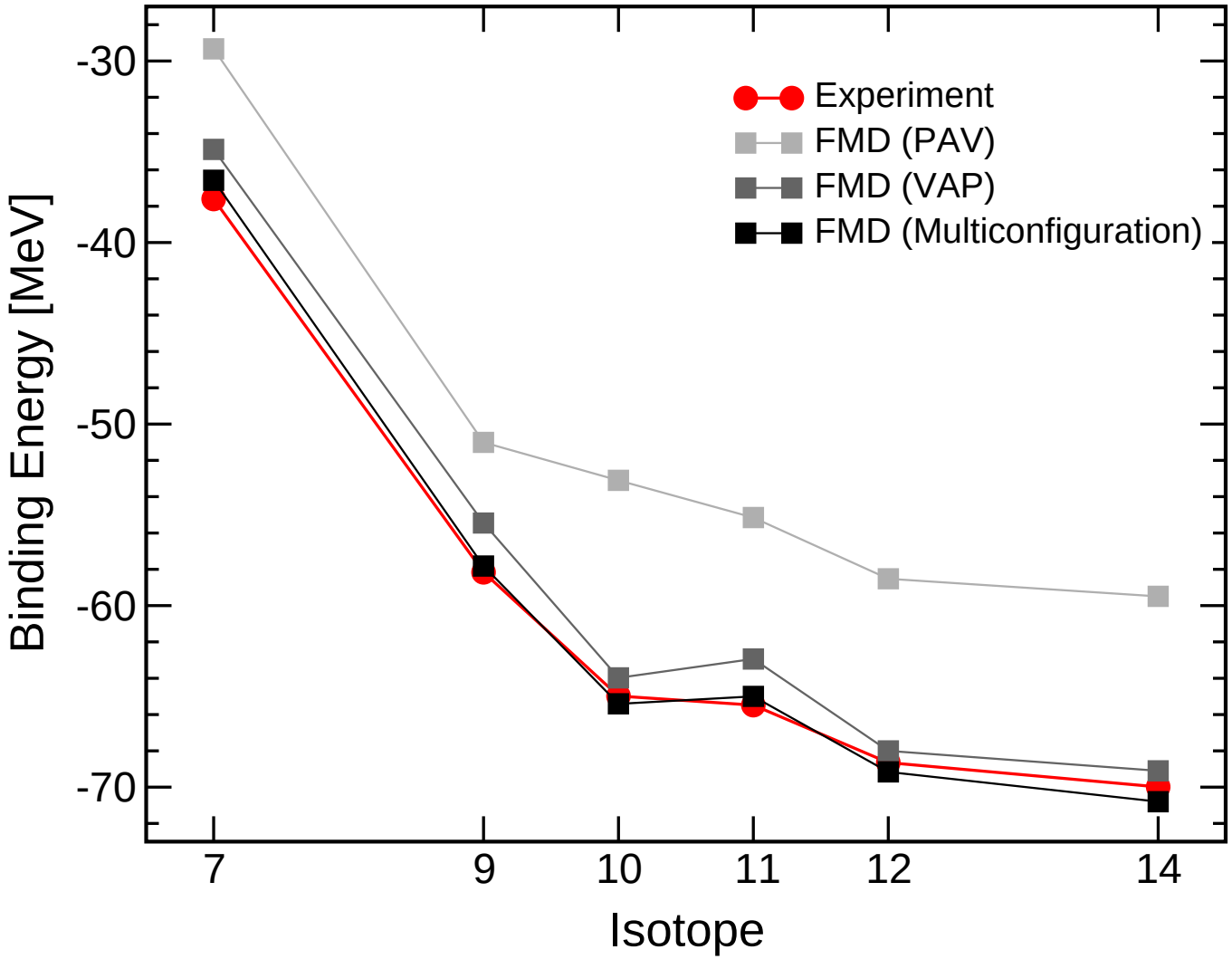

- large correlation energies due to cluster structure
- loosely bound systems gain most by configuration mixing

Beryllium Isotopes

$N = 8$ Shell Closure ?

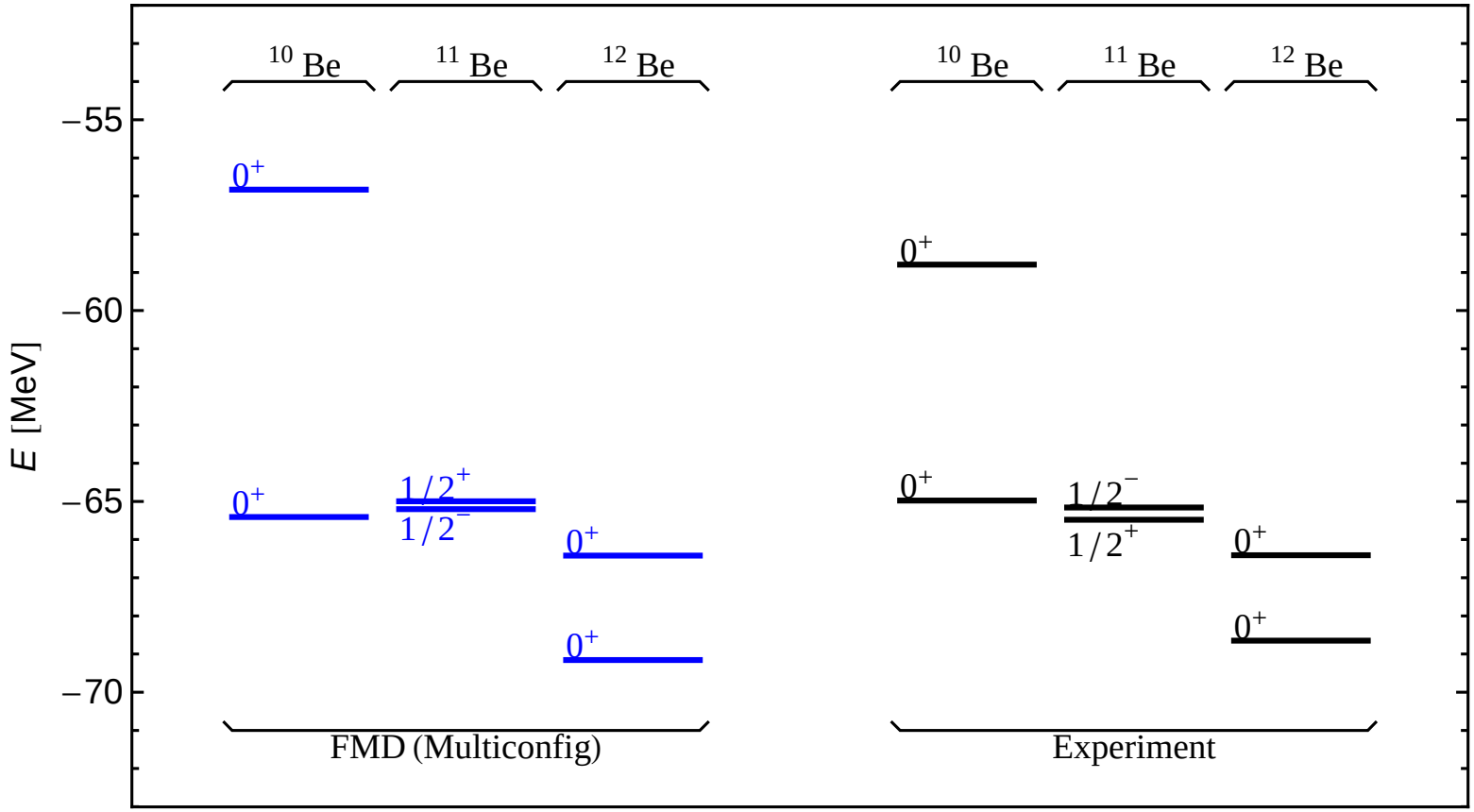

- "almost correct" level ordering in ^{11}Be
- ^{12}Be ground state dominated by p^2 configuration, sizeable admixture of s^2 and d^2 configurations which stronly mix

Beryllium Isotopes

Charge Radii

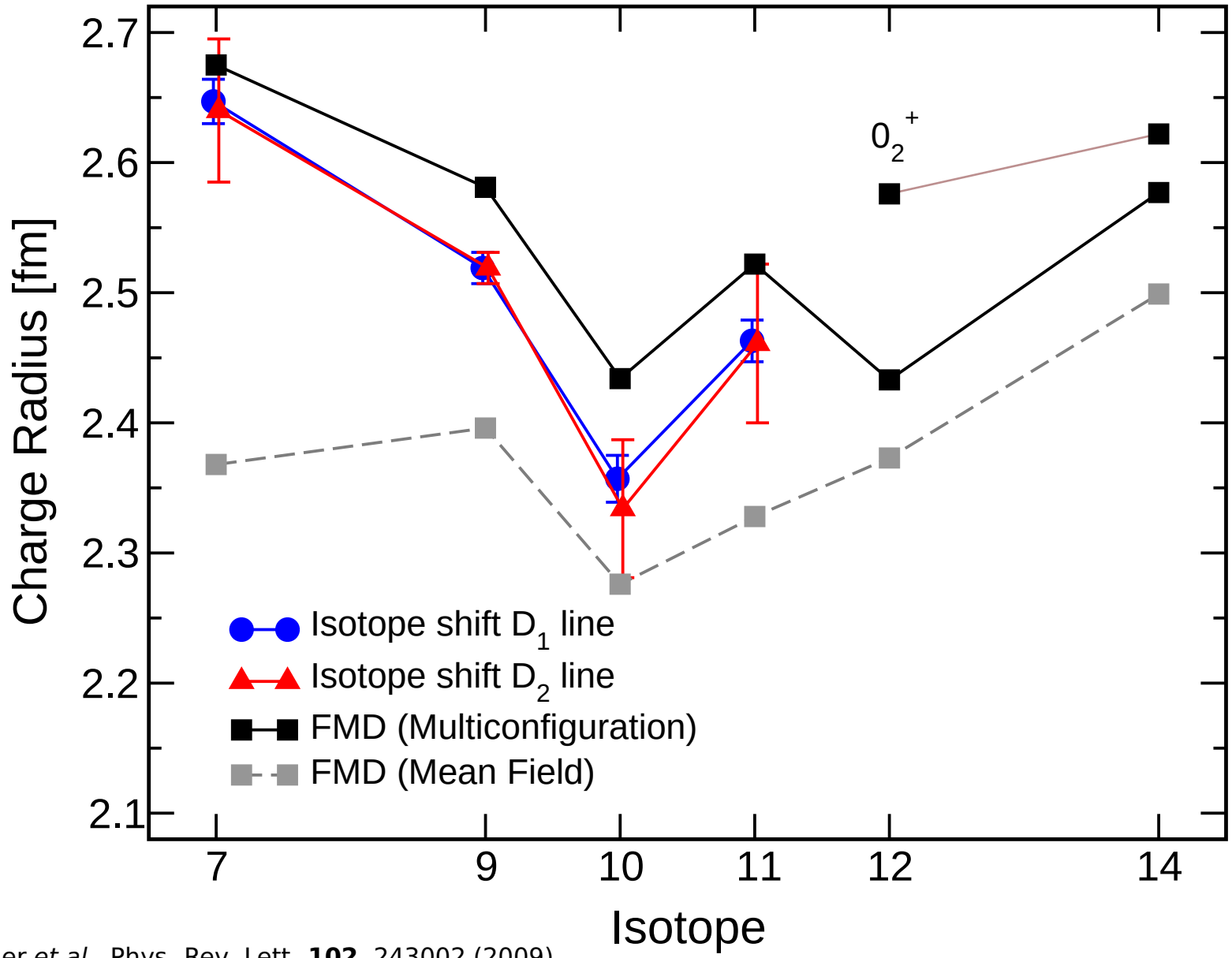

Nörtershäuser *et al.*, Phys. Rev. Lett. **102**, 243002 (2009)

Zakova, Neff, *et al.*, J. Phys. G, accepted for publication

Beryllium Isotopes

Matter Radii

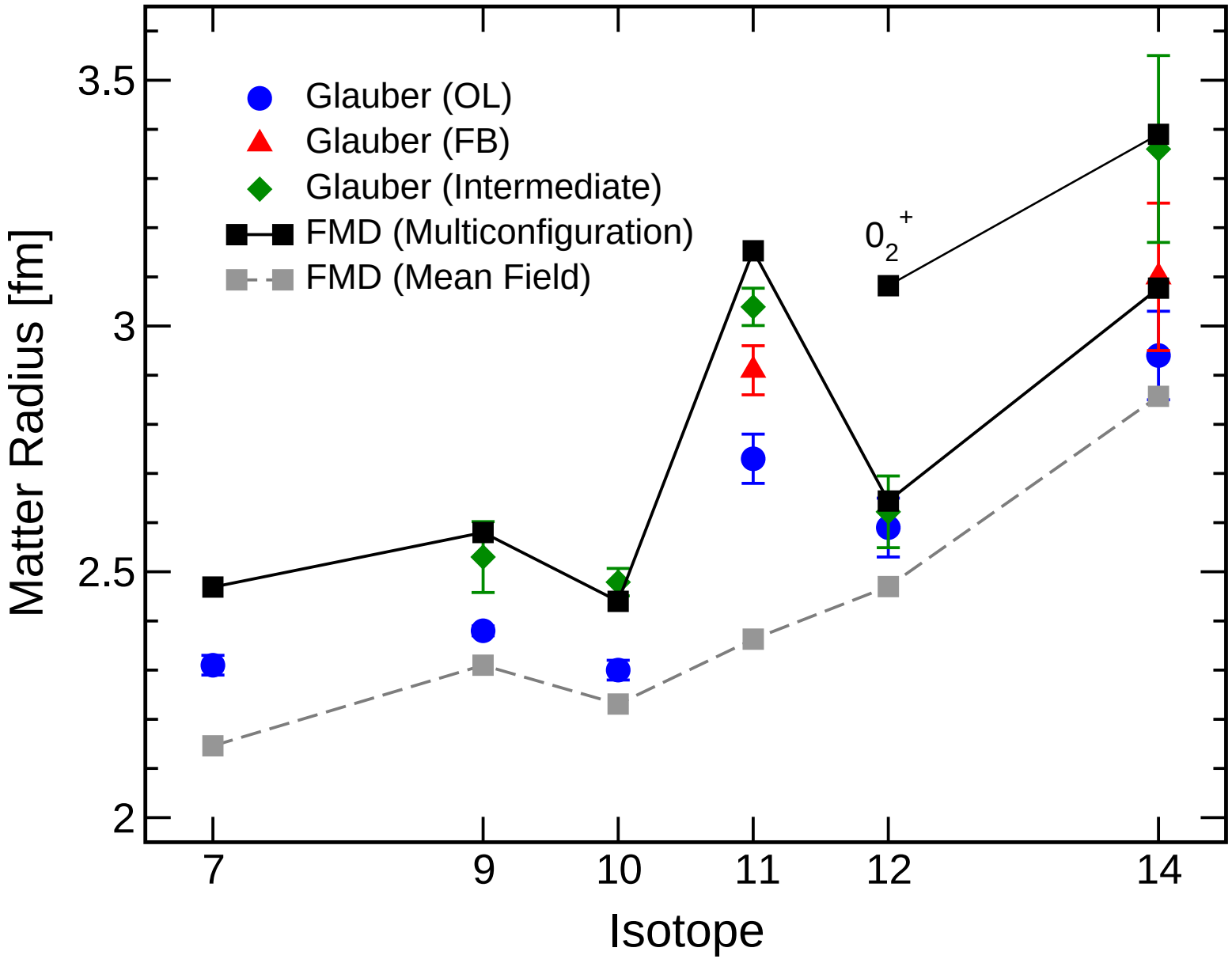

Ozawa *et al.*, Nucl. Phys. **A693**, 32 (2001).

Electromagnetic transitions

^{10}Be

	FMD(Multiconfig)	Experiment
$B(E2; 2_1^+ \to 0_1^+)$	11.27 e^2fm^4	9.2 ± 0.3 e^2fm^4
$B(E2; 2_2^+ \to 0_1^+)$	1.00 e^2fm^4	0.11 ± 0.02 e^2fm^4
$B(E2; 0_2^+ \to 2_1^+)$	4.99 e^2fm^4	3.2 ± 1.9 e^2fm^4
$B(E1; 0_2^+ \to 1_1^-)$	0.013 e^2fm^2	0.013 ± 0.004 e^2fm^2

^{11}Be

	FMD(Multiconfig)	Experiment
$B(E1; 1/2_1^+ \to 1/2_1^-)$	0.020 e^2fm^2	0.099 ± 0.010 e^2fm^2

^{12}Be

	FMD(Multiconfig)	Experiment
$B(E2; 2_1^+ \to 0_1^+)$	8.27 e^2fm^4	8.0 ± 3.0 e^2fm^4
$B(E2; 0_2^+ \to 2_1^+)$	6.50 e^2fm^4	7.0 ± 0.6 e^2fm^4
$M(E0; 0_1^+ \to 0_2^+)$	1.05 $e$fm^2	0.87 ± 0.03 $e$fm^2
$B(E1; 0_1^+ \to 1_1^-)$	0.08 e^2fm^2	0.051 ± 0.003 e^2fm^2

McCutchan *et al.*. Phys. Rev. Lett. **103**, 192501 (2009).
Nakamura *et al.*, Phys. Lett. **B394**, 11 (1997).
Shimoura *et al.*, Phys. Lett. **B654**, 87 (2007).

Iwasaki *et al.*, Phys. Lett. **B491**, 8 (2000).

^{11}Be-^{10}Be **Overlaps**

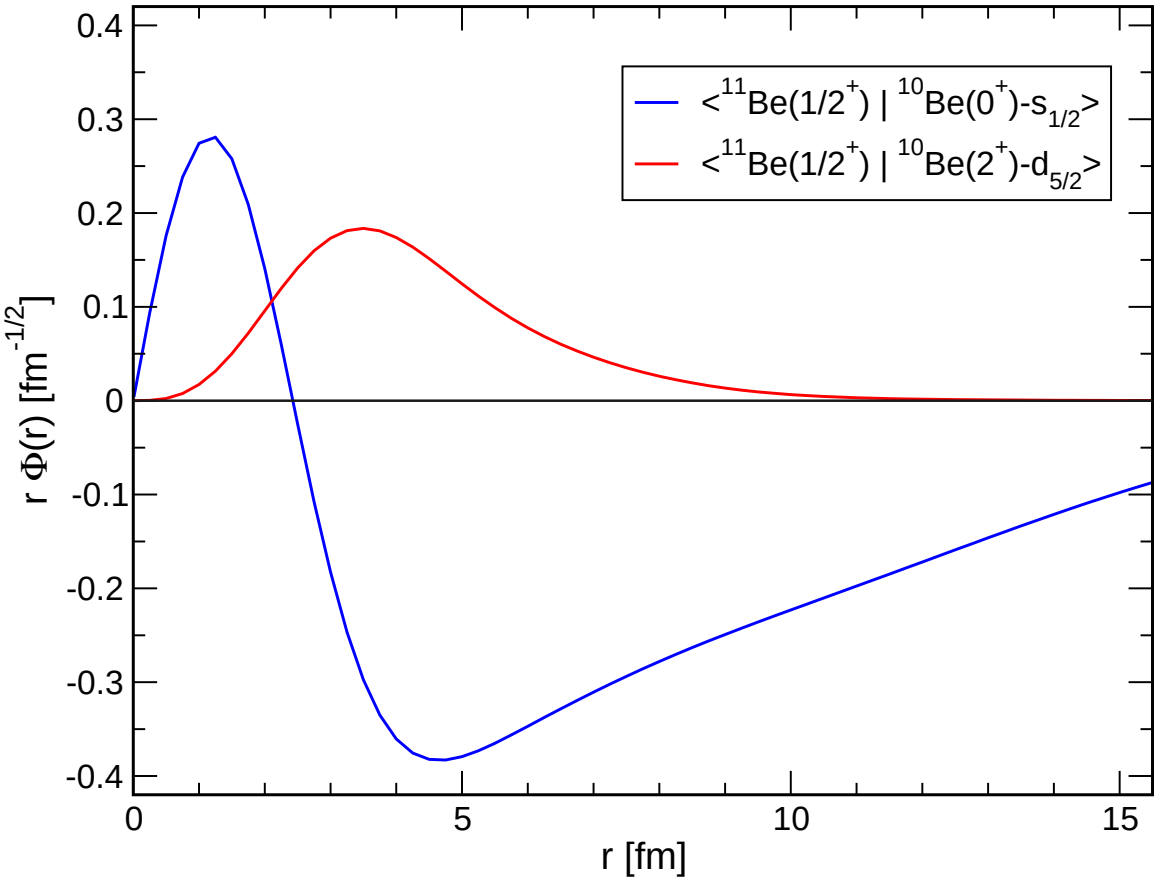

Spectroscopic Factors

^{11}Be	^{10}Be	l_j	S
$1/2^+$	0^+	$s_{1/2}$	0.937
	2^+	$d_{5/2}$	0.094
	2^+	$d_{3/2}$	0.007
$5/2^+$	0^+	$d_{5/2}$	0.543
	2^+	$s_{1/2}$	0.329
	2^+	$d_{5/2}$	0.243
$1/2^-$	0^+	$p_{1/2}$	0.805
	2^+	$p_{3/2}$	0.779

- extended *s*-wave halo
- $s_{1/2}$ spectroscopic factor larger than results obtained from knockout and transfer reactions

Cluster States in ^{12}C

Astrophysical Motivation

- **Helium burning: triple alpha-reaction**

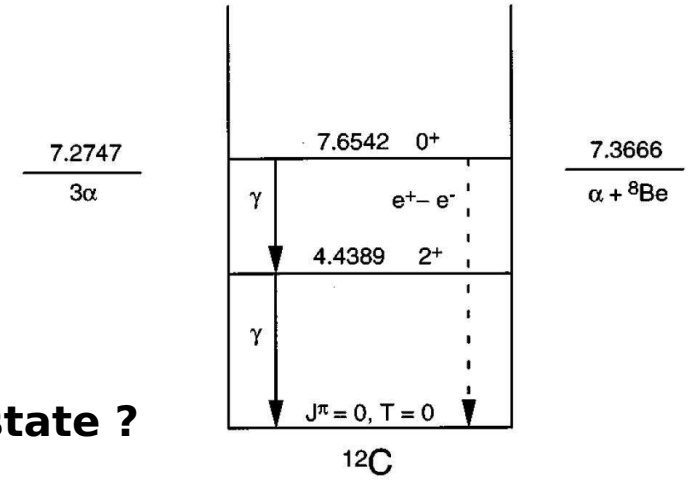

Structure

- **Is the Hoyle state a pure α-cluster state ?**
- **Other excited 0^+ and 2^+ states**

➨ **Compare FMD results to microscopic α-cluster model**

➨ **Analyze wave functions in harmonic oscillator basis**

➨ **No-Core Shell Model Calculations ?**

Cluster States in ^{12}C

Triple α Reaction

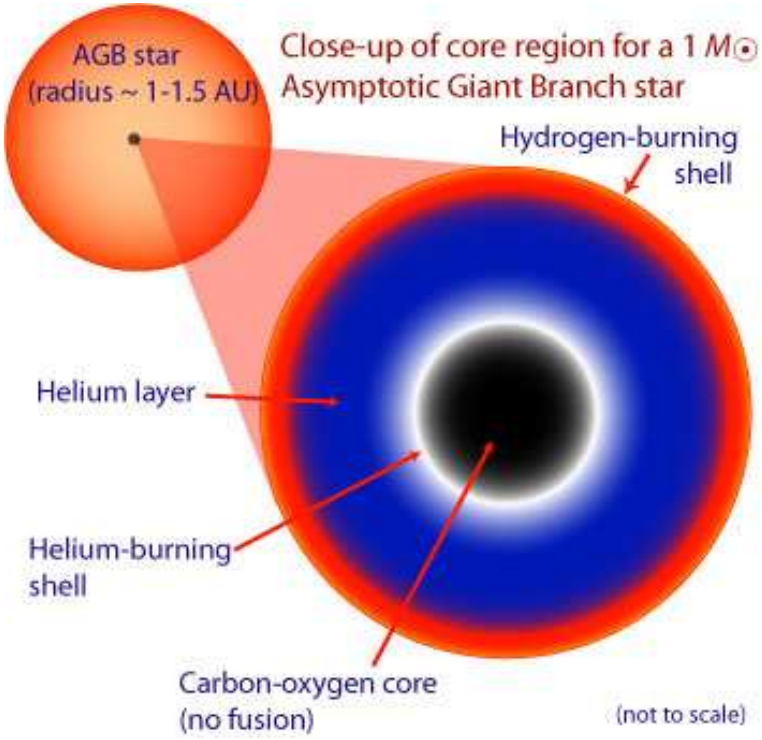

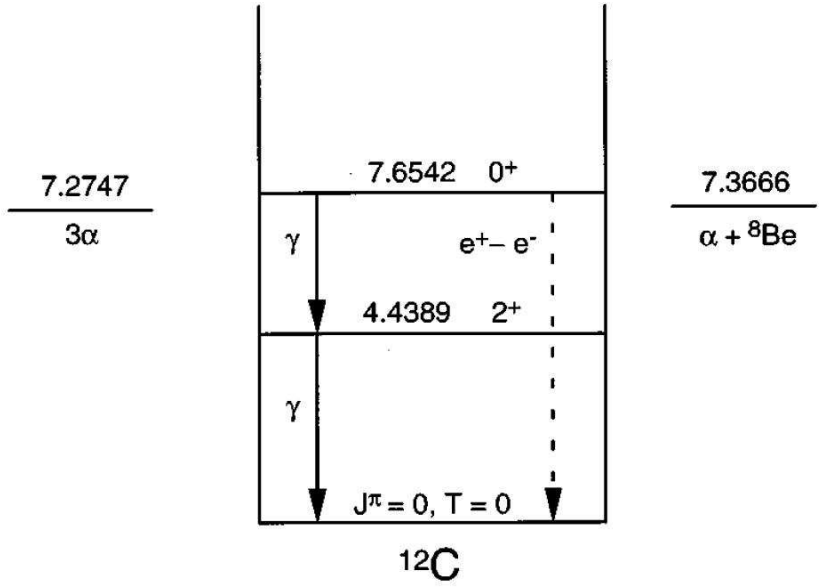

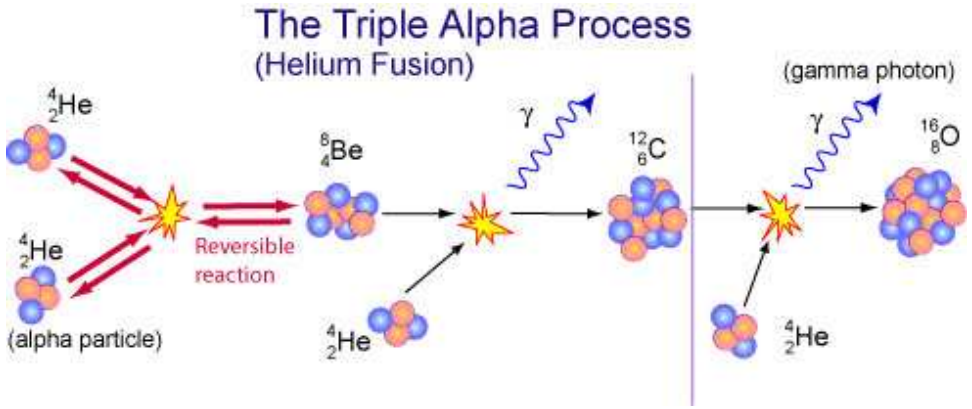

http://outreach.atnf.csiro.au/education/senior/astrophysics/stellarevolution_postmain.html

Cluster States in ^{12}C

Microscopic α-Cluster Model

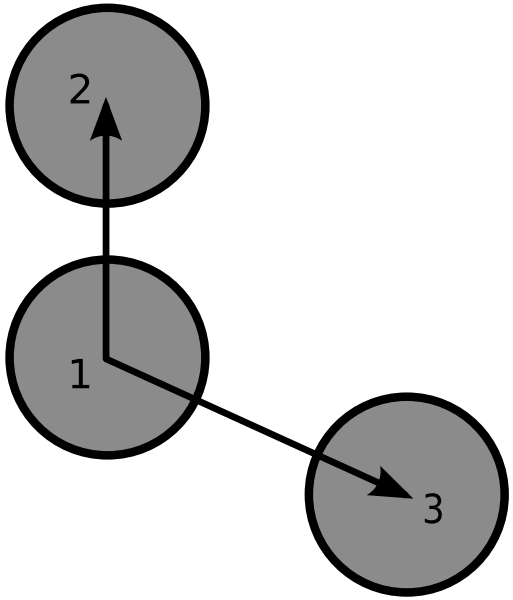

$$R_{12} = (2, 4, \ldots, 10)\,\text{fm}$$
$$R_{13} = (2, 4, \ldots, 10)\,\text{fm}$$
$$\cos(\vartheta) = (1.0, 0.8, \ldots, -1.0)$$

alltogether 165 configurations

Basis States

- describe Hoyle State as a system of 3 ^{4}He nuclei

$$\left|\Psi_{3\alpha}(\mathbf{R}_1, \mathbf{R}_2, \mathbf{R}_3); JMK\pi\right\rangle = P^J_{MK} P^\pi \mathcal{A}\left\{\left|\psi_\alpha(\mathbf{R}_1)\right\rangle \otimes \left|\psi_\alpha(\mathbf{R}_2)\right\rangle \otimes \left|\psi_\alpha(\mathbf{R}_3)\right\rangle\right\}$$

Volkov Interaction

- simple central interaction
- parameters adjusted to reproduce α binding energy and radius, $\alpha - \alpha$ scattering data and C12 ground state energy

✘ only reasonable for ^{4}He, ^{8}Be and ^{12}C nuclei

'BEC' wave functions

- interpretation of the Hoyle state as a Bose-Einstein Condensate of α-particles by Funaki, Tohsaki, Horiuchi, Schuck, Röpke
- same interaction and α-cluster parameters used

Kamimura, Nuc. Phys. **A351** (1981) 456

Funaki et al., Phys. Rev. C **67** (2003) 051306(R)

FMD

Basis States

- 20 FMD states obtained in Variation after Projection on 0^+ and 2^+ with constraints on the radius
- 42 FMD states obtained in Variation after Projection on parity with constraints on radius and quadrupole deformation
- 165 α-cluster configurations

➨ projected on angular momentum and linear momentum

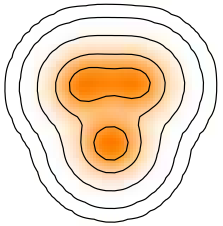

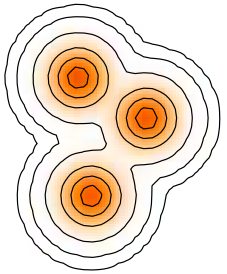

Interaction

- not tuned for α-α scattering or ^{12}C properties

Cluster States in ^{12}C
α-α Phaseshifts

FMD

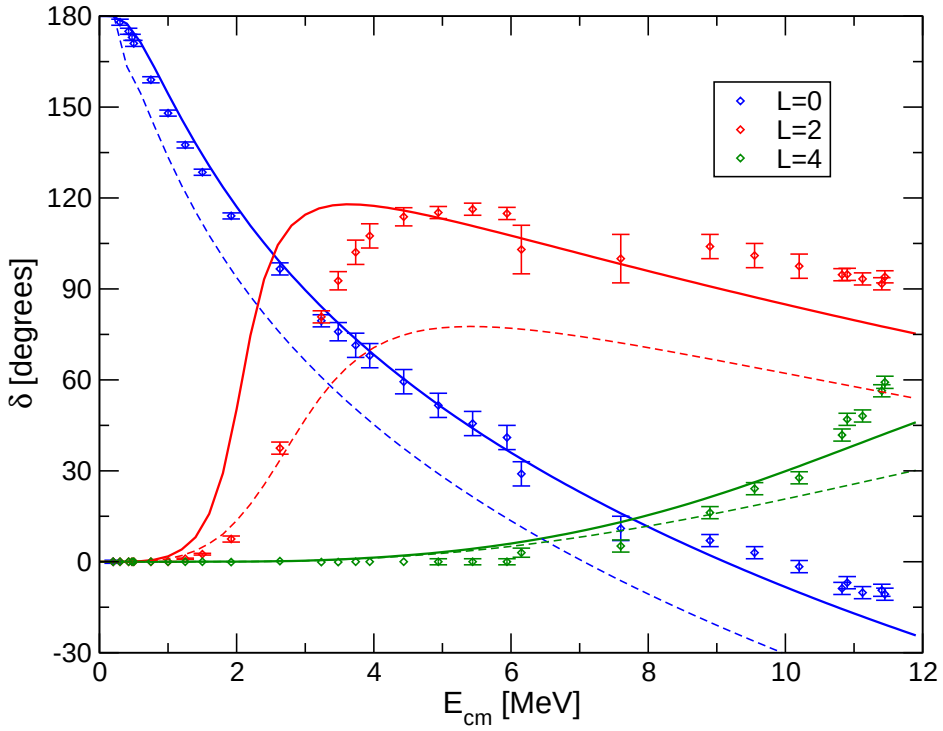

Cluster Model

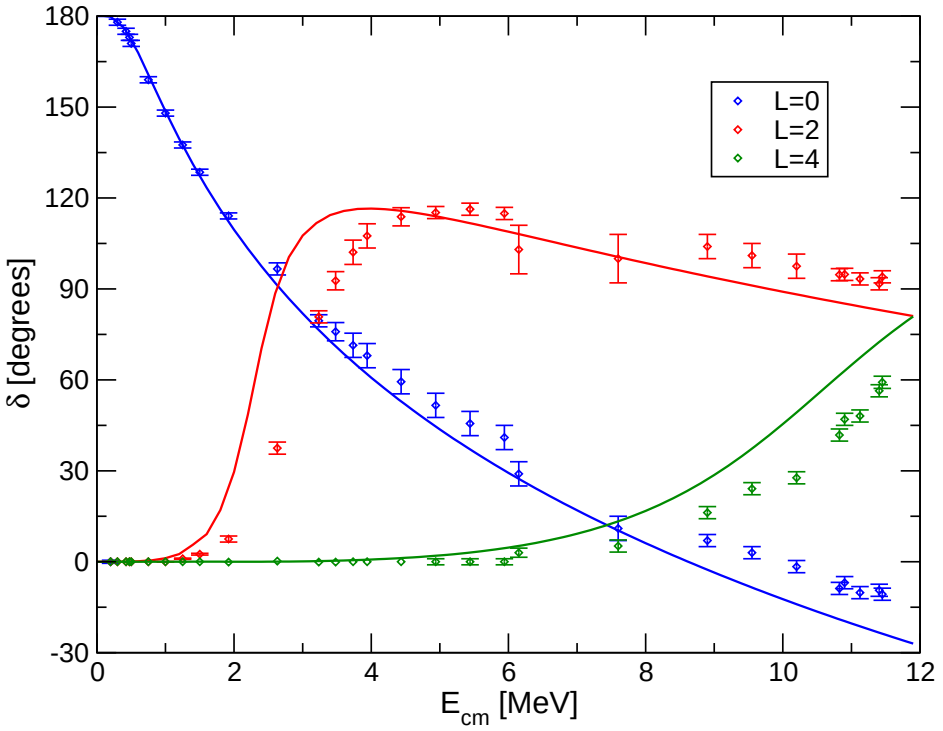

- Phaseshifts calculated with cluster configurations only (dashed lines)
- Phaseshifts calculated with additional FMD VAP configurations in the interaction region (solid lines)

- only cluster configurations included

➨ similar quality for description of α-α-scattering

Cluster States in ^{12}C
Comparison

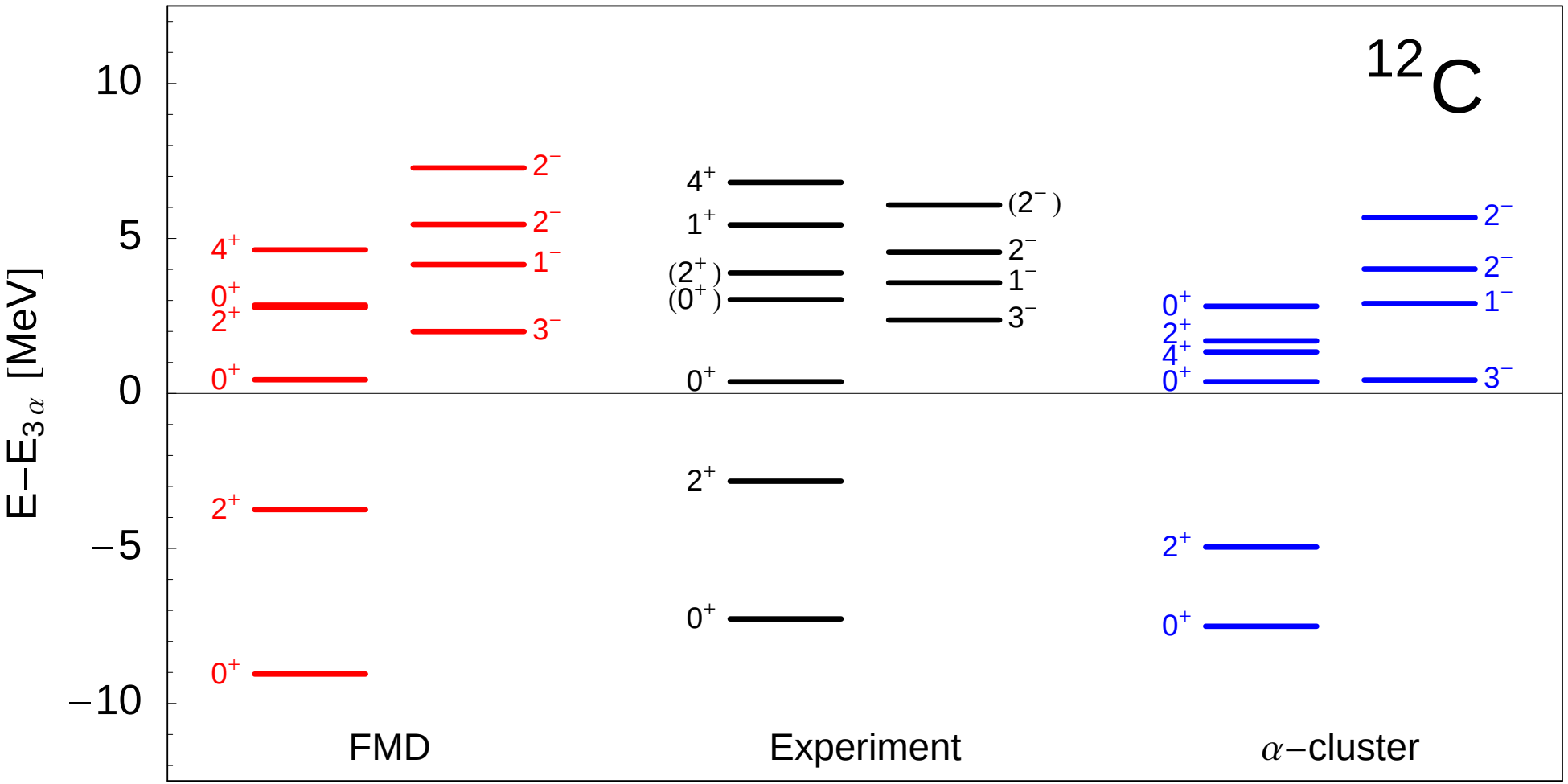

Cluster States in ^{12}C
Comparison

	Exp[1]	Exp[2]	Exp[3]	FMD	α-cluster	'BEC'[4]
$E(0_1^+)$	-92.16			-92.64	-89.56	-89.52
$E^*(2_1^+)$	4.44			5.31	2.56	2.81
$E(3\alpha)$	-84.89			-83.59	-82.05	-82.05
$E(0_2^+) - E(3\alpha)$	0.38			0.43	0.38	0.26
$E(0_3^+) - E(3\alpha)$	(3.0)	2.7(3)	3.96(5)	2.84	2.81	
$E(2_2^+) - E(3\alpha)$	(3.89)	2.6(3)	6.63(3)	2.77	1.70	
$r_{\text{charge}}(0_1^+)$	2.47(2)			2.53	2.54	
$r(0_1^+)$				2.39	2.40	2.40
$r(0_2^+)$				3.38	3.71	3.83
$r(0_3^+)$				4.62	4.75	
$r(2_1^+)$				2.50	2.37	2.38
$r(2_2^+)$				4.43	4.02	
$M(E0, 0_1^+ \to 0_2^+)$	5.4(2)			6.53	6.52	6.45
$B(E2, 2_1^+ \to 0_1^+)$	7.6(4)			8.69	9.16	
$B(E2, 2_1^+ \to 0_2^+)$	2.6(4)			3.83	0.84	

experimental situation for 0_3^+ and 2_2^+ states still unsettled

2_2^+ resonance at 1.8 MeV above treshold included in NACRE compilation

[1] Ajzenberg-Selove, Nuc. Phys. **A506**, 1 (1990)
[2] Itoh et al., Nuc. Phys. **A738**, 268 (2004)
[3] Fynbo et al., Nature **433**, 137 (2005). Diget et al., Nuc. Phys. **A738**, 760 (2005)
[4] Funaki et al., Phys. Rev. C **67**, 051306(R) (2003)

Cluster States in ^{12}C
Comparison

	Exp[1]	Exp[2]	Exp[3]	FMD	α-cluster	'BEC'[4]
$E(0_1^+)$	-92.16			-92.64	-89.56	-89.52
$E^*(2_1^+)$	4.44			5.31	2.56	2.81
$E(3\alpha)$	-84.89			-83.59	-82.05	-82.05
$E(0_2^+) - E(3\alpha)$	0.38			0.43	0.38	0.26
$E(0_3^+) - E(3\alpha)$	(3.0)	2.7(3)	3.96(5)	2.84	2.81	
$E(2_2^+) - E(3\alpha)$	(3.89)	2.6(3)	6.63(3)	2.77	1.70	
$r_{\text{charge}}(0_1^+)$	2.47(2)			2.53	2.54	
$r(0_1^+)$				2.39	2.40	2.40
$r(0_2^+)$				3.38	3.71	3.83
$r(0_3^+)$				4.62	4.75	
$r(2_1^+)$				2.50	2.37	2.38
$r(2_2^+)$				4.43	4.02	
$M(E0, 0_1^+ \to 0_2^+)$	5.4(2)			6.53	6.52	6.45
$B(E2, 2_1^+ \to 0_1^+)$	7.6(4)			8.69	9.16	
$B(E2, 2_1^+ \to 0_2^+)$	2.6(4)			3.83	0.84	

experimental situation for 0_3^+ and 2_2^+ states still unsettled

2_2^+ resonance at 1.8 MeV above treshold included in NACRE compilation

calculated in bound state approximation

➨ include ^{8}Be+^{4}He channels for two-body decay

[1] Ajzenberg-Selove, Nuc. Phys. **A506**, 1 (1990)
[2] Itoh et al., Nuc. Phys. **A738**, 268 (2004)
[3] Fynbo et al., Nature **433**, 137 (2005). Diget et al., Nuc. Phys. **A738**, 760 (2005)
[4] Funaki et al., Phys. Rev. C **67**, 051306(R) (2003)

Cluster States in ^{12}C

Electron Scattering Data

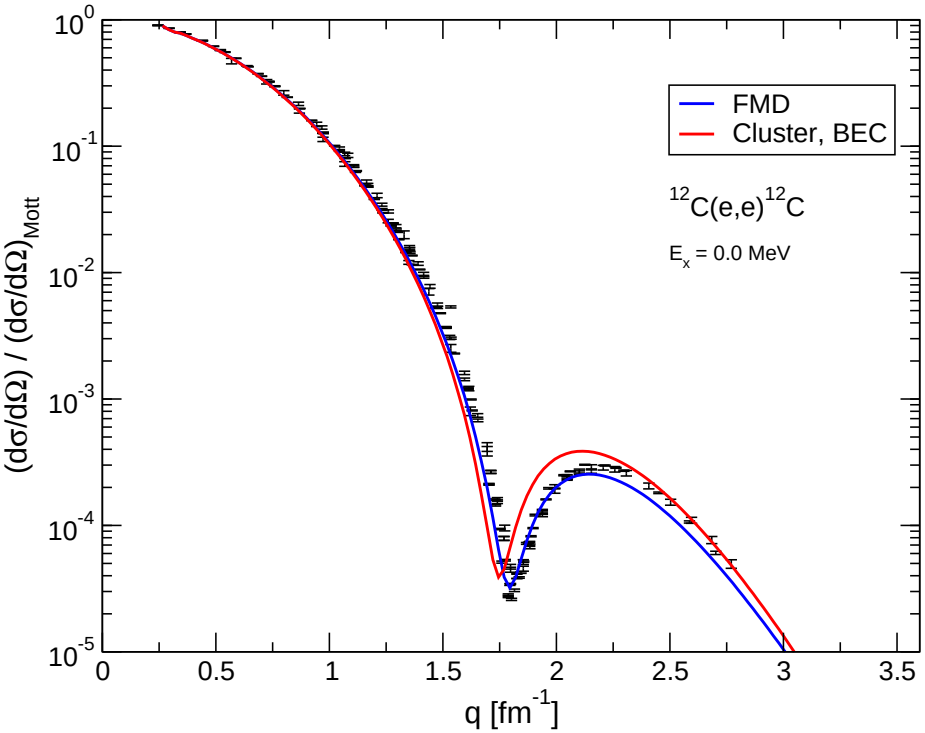

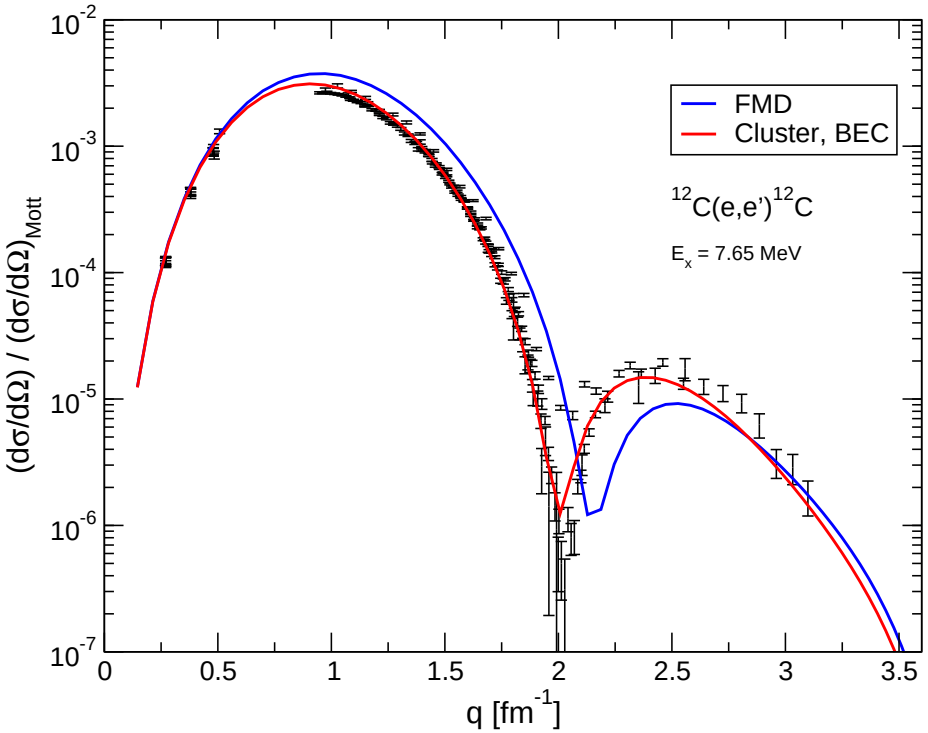

- compare with precise electron scattering data up to high momenta in Distorted Wave Born Approximation
- use intrinsic density

$$\rho(\mathbf{x}) = \sum_{k=1}^{A} \langle \Psi \left| \delta(\underset{\sim}{\mathbf{x}}_k - \underset{\sim}{\mathbf{X}} - \mathbf{x}) \right| \Psi \rangle$$

- elastic cross section described very well by FMD
- transition cross section better described by cluster model

M. Chernykh, H. Feldmeier, T. Neff, P. von Neumann-Cosel, and A. Richter, Phys. Rev. Lett. **98** (2007) 032501

Cluster States in ^{12}C

Important Configurations

- Calculate the overlap with FMD basis states to find the most important contributions to the Hoyle state

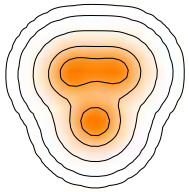

$\left|\left\langle \cdot \mid 0_1^+ \right\rangle\right| = 0.94$

$\left|\left\langle \cdot \mid 2_1^+ \right\rangle\right| = 0.93$

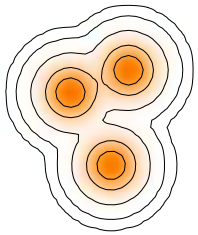

$\left|\left\langle \cdot \mid 0_2^+ \right\rangle\right| = 0.72$

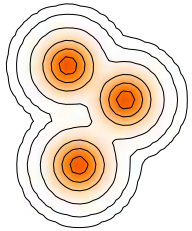

$\left|\left\langle \cdot \mid 0_2^+ \right\rangle\right| = 0.71$

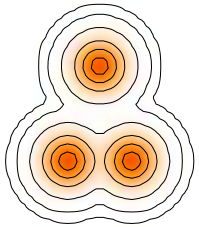

$\left|\left\langle \cdot \mid 0_2^+ \right\rangle\right| = 0.61$

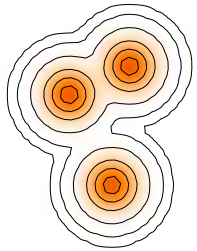

$\left|\left\langle \cdot \mid 0_2^+ \right\rangle\right| = 0.61$

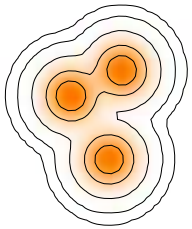

$\left|\left\langle \cdot \mid 3_1^- \right\rangle\right| = 0.83$

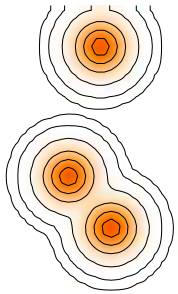

$\left|\left\langle \cdot \mid 0_3^+ \right\rangle\right| = 0.50$

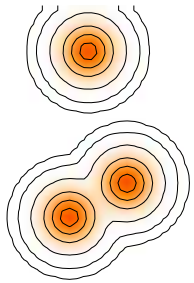

$\left|\left\langle \cdot \mid 0_3^+ \right\rangle\right| = 0.49$

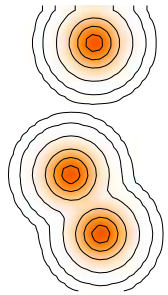

$\left|\left\langle \cdot \mid 0_3^+ \right\rangle\right| = 0.44$

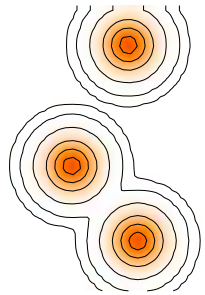

$\left|\left\langle \cdot \mid 0_3^+ \right\rangle\right| = 0.41$

FMD basis states are not orthogonal!

loosely bound, gas-like states

Cluster States in ^{12}C

Overlap with Cluster Model Space

Calculate the overlap of FMD wave functions with pure α-cluster model space

$$N_\alpha = \langle \Psi \left| \underset{\sim}{P}_{3\alpha} \right| \Psi \rangle$$

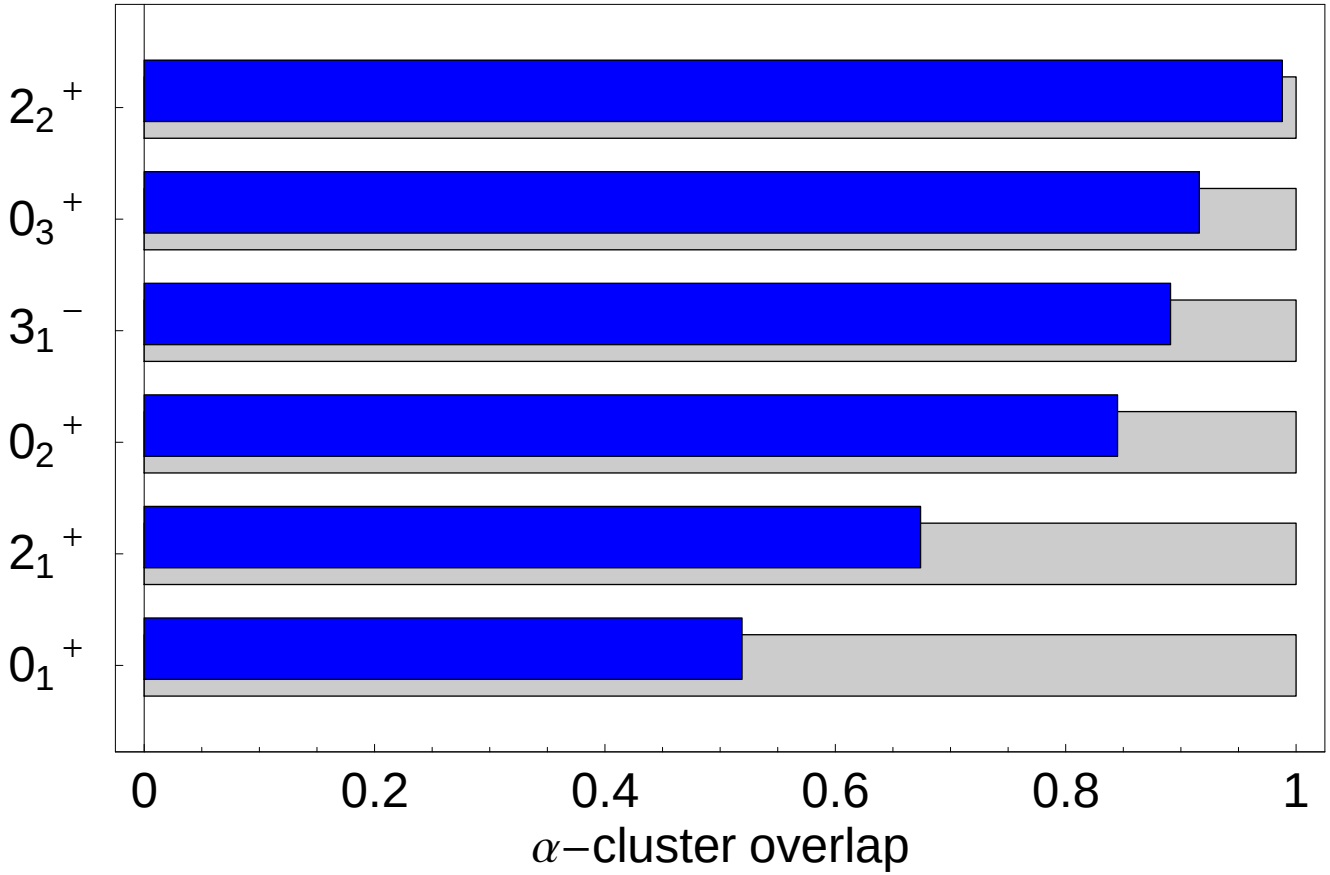

Hoyle state has 15% non-alpha admixtures

Cluster States in ^{12}C
Harmonic Oscillator $N\hbar\Omega$ Excitations

Y. Suzuki et al., Phys. Rev. C **54** (1996) 2073

$$\mathrm{Occ}(N) = \langle \Psi \left| \delta \left(\sum_i (\underset{\sim}{H}_i^{HO}/\hbar\Omega - 3/2) - N \right) \right| \Psi \rangle$$

FMD

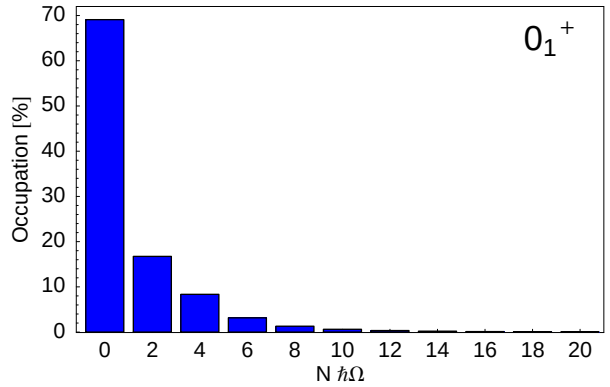

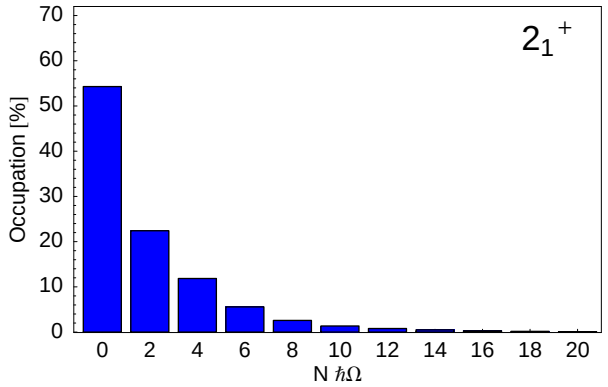

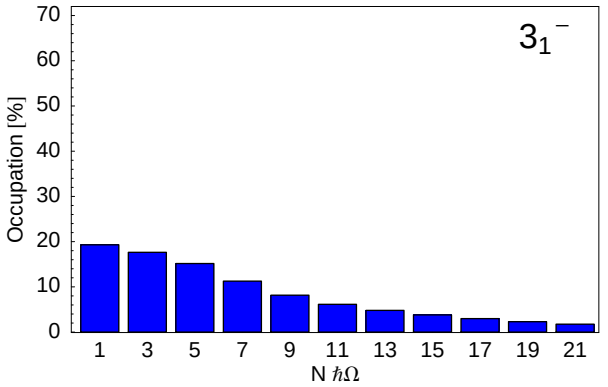

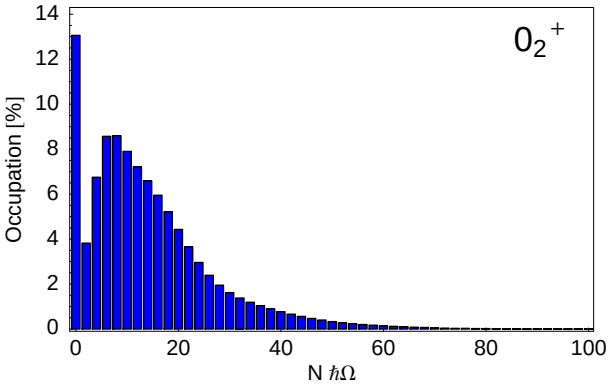

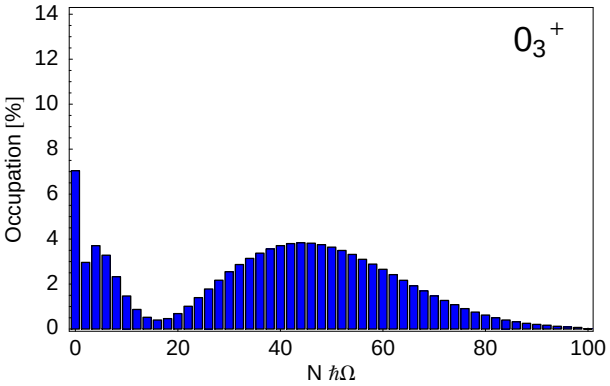

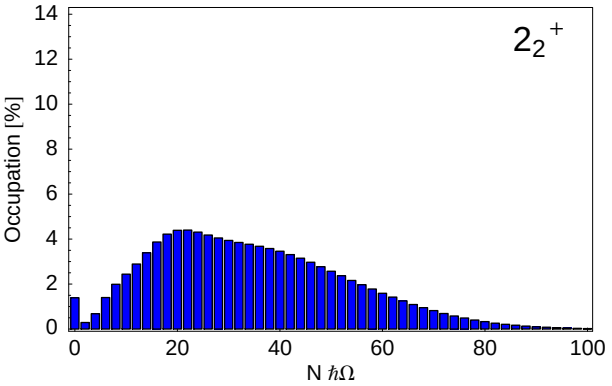

Cluster States in ^{12}C
Harmonic Oscillator $N\hbar\Omega$ Excitations

Y. Suzuki *et al*, Phys. Rev. C **54**, 2073 (1996).

$$\mathrm{Occ}(N) = \langle \Psi \left| \delta \left(\sum_i (\underset{\sim}{H}_i^{HO}/\hbar\Omega - 3/2) - N \right) \right| \Psi \rangle$$

Cluster Model

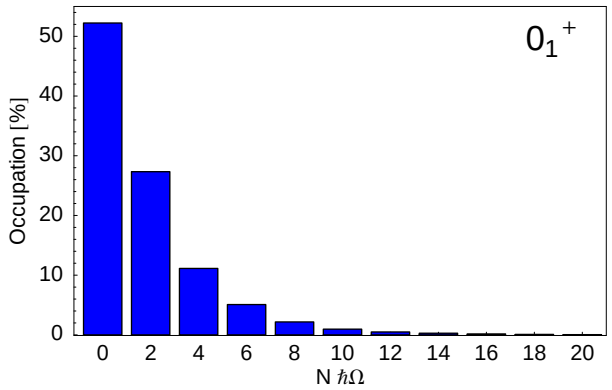

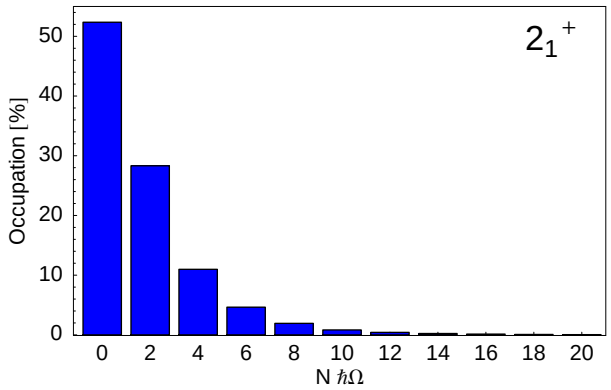

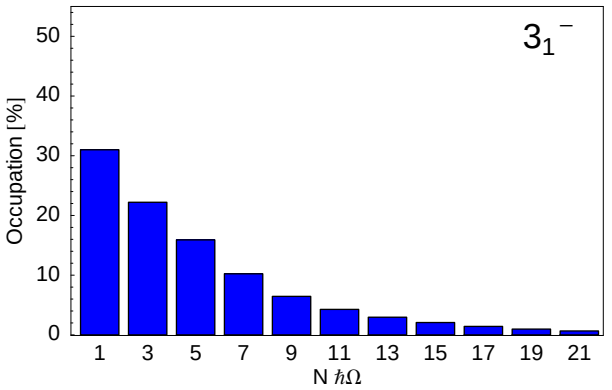

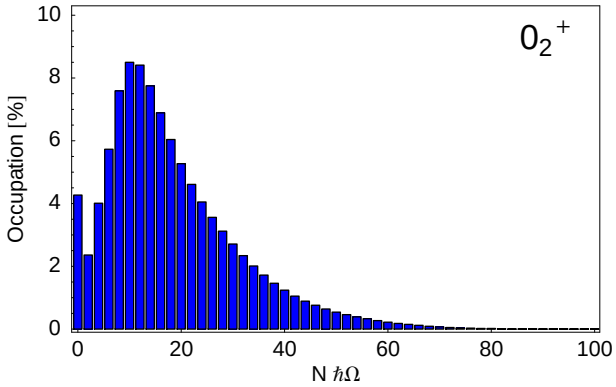

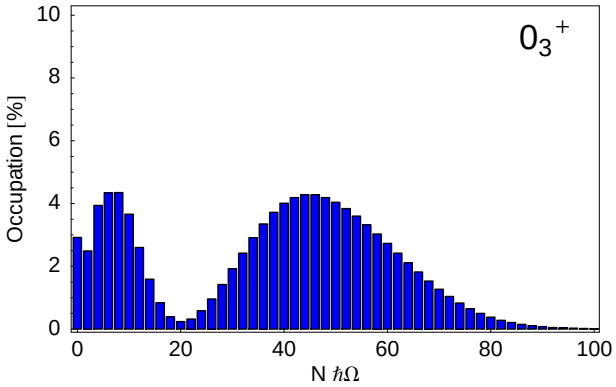

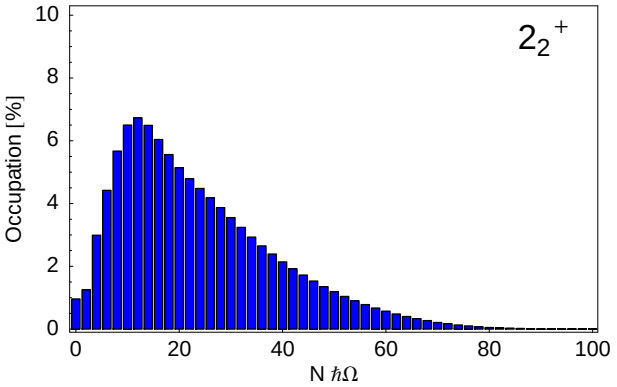

Cluster States in ^{12}C

α-cluster states in the No-Core Shell Model ?

- compare spectra in NCSM and α-cluster model using the Volkov interaction
- bare interaction used in NCSM calculations

➨ good agreement for ground state band (0^+_1, 2^+_1, 4^+_1)

➨ very slow convergence for cluster states

Binding energies

	^{4}He	^{12}C
Cluster	-27.3 MeV	-89.6 MeV
NCSM	-28.3 MeV	-95.4 MeV

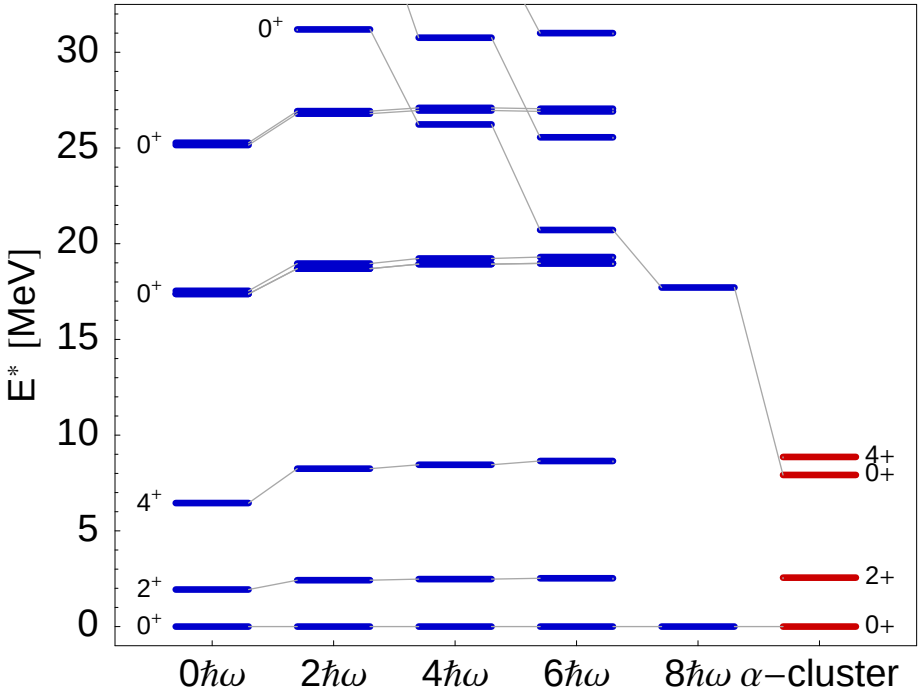

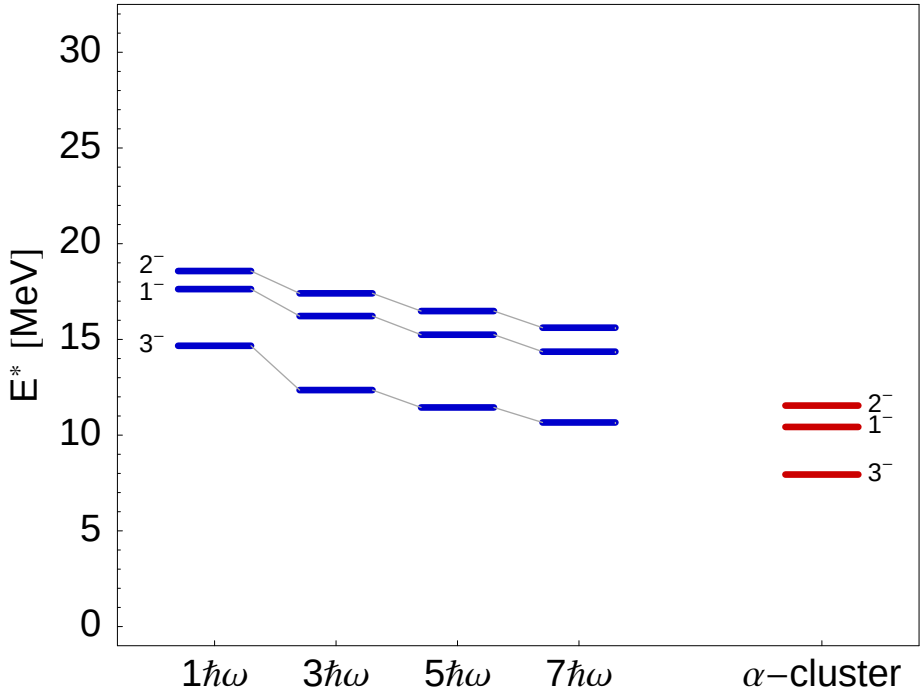

Cluster States in ^{12}C

α-cluster states in the No-Core Shell Model ?

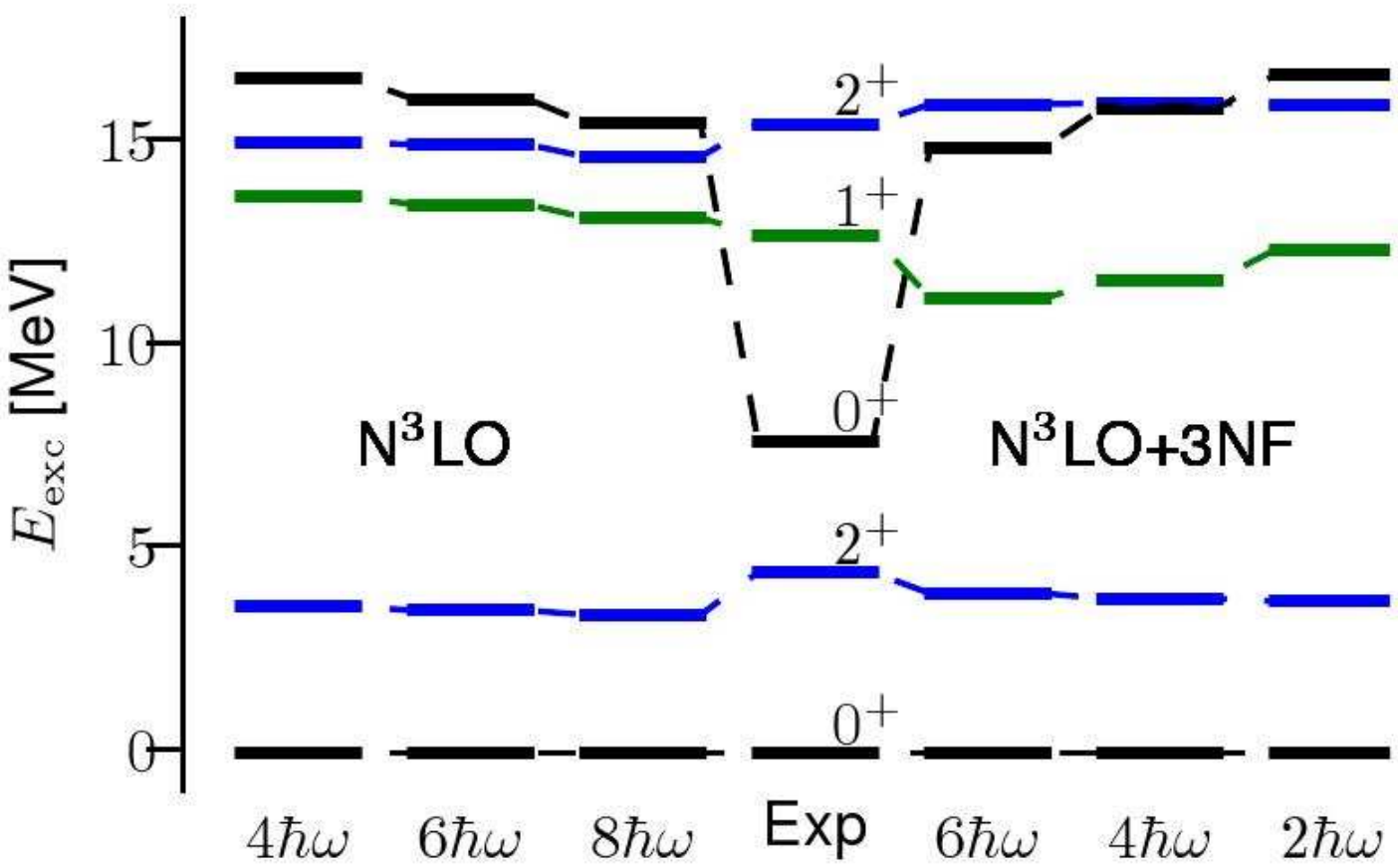

➨ three-body forces do not help !

Navrátil, Gueorgiev, Vary, Ormand, Nogga, Phys. Rev. Lett. **99** (2007) 042501

Advantages/Disadvantages of FMD approach

FMD vs *ab initio*

Advantages

- basis very flexible, clusters and halo structure can be described
- can be used for light *p*/*sd*-shell nuclei
- many observables can be calculated
- intrinsic states provide an “intuitive” picture of the nucleus

Disadvantages

- interaction has to be soft and given in operator representation
- does not provide “exact” results for given interaction, not straightforward to check convergence by “increasing model space size”

FMD vs few-body models

Advantages

- microscopic - antisymmetrization
- cluster structure appears naturally, includes polarization effects
- uses nucleon-nucleon interaction, no need for phenomenological potentials

Disadvantages

- numerical effort, “exact” calculations are not possible
- not possible to adjust thresholds ”by hand"
- much more difficult to include boundary conditions for resonance or scattering states

Thanks

to my Collaborators

S. Bacca, A. Cribeiro, R. Cussons, H. Feldmeier, P. J. Ginsel, B. Hellwig, K. Langanke, R. Torabi, D. Weber

GSI Darmstadt

H. Hergert, R. Roth

Institut für Kernphysik, TU Darmstadt